

**GAS PHASE ACIDITY AND PROTON AFFINITY STUDIES OF ORGANIC
SPECIES USING MASS SPECTROMETRY**

By

SISI ZHANG

A thesis submitted to the

Graduate School-New Brunswick

Rutgers, The State University of New Jersey

in partial fulfillment of the requirements

for the degree of

Master of Science

Graduate Program in Chemistry and Chemical Biology

written under the direction of

Professor's Jeehiun K. Lee

and approved by

New Brunswick, New Jersey

[October, 2012]

ABSTRACT OF THE THESIS

GAS PHASE ACIDITY AND PROTON AFFINITY STUDIES OF ORGANIC SPECIES USING MASS SPECTROMETRY

By SISI ZHANG

Thesis Director:

Professor Jeehiun K. Lee

DNA damaged bases are one of the reasons for a variety diseases, such as carcinogenesis, aging and cell death. uracil is a nucleobase that arises from cytosine deamination. *N*-Deprotonated uracil functions as a leaving group during the deamination process. Theoretically, in the S_N2 reaction, leaving group ability tracks with pK_a of the conjugate acid in the solution phase, that is, lower pK_a is associated with better leaving group ability. In the gas phase, leaving group ability is better with higher acidity of the conjugate acid. The studies we did previously showed that although 3-methyluracil is as acidic as hydrochloric acid in the gas phase, the leaving group ability of chloride is better than deprotonated 3-methyluracil. The reason we propose this is that the electron delocalization in the transition state of S_N2 reaction cannot be fully recognized as in

acidity. Therefore, we designed substituted aniline and amine with leaving groups with or without the ability of electron delocalization and found that substituted amine with leaving groups that did not have the ability of electron delocalization tracked better with acidity than the one with the ability of electron delocalization. The result is consistent with our proposal. We also tested the Hammond postulate with the calculation results.

Another focus of interest is N-heterocyclic singlet carbenes (NHCs), which are ligands of a variety of organometallic catalysts. Presumably the ligands are more effective if they are more basic, that is, with higher proton affinity. The protonated carbenes are also an important class of ionic liquids, known as green solvents with several advantages over traditional organic solvents. Strassner *et al* designed a new type of ionic liquid imidazolium salt with tunable para-aryl substituent, and we measured the acidity of these tunable aryl-alkyl ionic liquids (TAAILs).

The proton-bound dimers of dimethyl imidazole and PCy₃ are found to exhibit interesting reactivity. In addition to producing just protonated carbenes and protonated phosphine with collision induced dissociation (CID), the proton-bound dimers generate another ion of interest with m/z 295. We designed and synthesized the di-CD₃ imidazole, and proved that the dimethyl system undergoes phosphine methylation during CID process.

ACKNOWLEDGEMENTS

I would like to express my sincere appreciation to my advisor, Dr. Jeehiun K. Lee, for all her help and suggestions for these years. I would also like to thank Dr. Romsted and Dr. Jimenze in Chemistry and Chemical Biology Department, to be my committee and their time and helpful suggestions. Special thanks to Dr. Strassner in Germany for his collaboration.

I would like to thank the previous and current members of Lee group: Min Liu, Anna Michelson, Mu Chen, Kai Wang, Sisi Zhang, Yuan Tian, Pingcheng Chu and Hao Zeng for their friendship and help in both research and life.

I am very grateful to my parents and friends for their unconditional support and love at every step of my life.

TABLE OF CONTENTS

ABSTRACT OF THE THESIS	ii
ACKNOWLEDGEMENTS	iv
TABLE OF CONTENTS	v
LIST OF FIGURES	vii
LIST OF TABLES	ix
Chapter 1 Introduction.....	1
1.1 Overview	1
1.1.1 Gas phase acidity and proton affinity	1
1.1.2 Gas phase thermochemical property study of substituted aniline and amine	2
1.1.3 Gas phase proton affinity of N-heterocyclic carbenes (NHCs)	2
1.2 Instrumentation.....	2
1.2.1 FTMS.....	2
1.2.2 ESI and ion trap mass spectrometer	4
1.3 Methodology	6
1.3.1 Bracketing method in FTMS	6
1.3.2 Bracketing method in LCQ.....	8
1.3.3 Cooks Kinetic Method.....	9
1.3.4 Calculations	10
Chapter 2 S_N2 project.....	11
2.1 Introduction	11
2.2 Experimental	12

2.3 Results	15
2.3.1 Computational results: acidities, ΔH^\ddagger	15
2.3.2 Computational results: r_1 , r_2	20
2.3.3 Experimental results: acidities.....	24
2.3.4 Experimental results: S_N2 (tert-butyl methyl(phenyl)carbamate)	26
2.3.5 Experimental results: S_N2 (N, N-dimethylacrylamide)	28
2.4 Discussion & Conclusion	29
2.4.1 Relationship of leaving group ability and acidity	29
2.4.2. Hammond postulate	29
Chapter 3 Strassner carbene project	31
3.1 Introduction	31
3.2 Experimental	33
3.2.1 Bartberger's method.....	33
3.2.2 Ogretir's method.....	33
3.3 Results	34
3.3.1 Calculation results: proton affinity	34
3.3.2 Calculation results: pK_a (Bartberger's method).....	35
3.3.3 Calculation results: pK_a (Ogretir's method)	40
3.3.4 Experimental results: proton affinity	45
3.4 Discussion & Conclusion	47
Chapter 4 Stabilized carbene project.....	49
4.1 Introduction	49
4.2 Experimental	51
4.3 Results	52
4.4 Conclusion.....	53
Reference	54
CURRICULUM VITAE.....	57

LIST OF FIGURES

Figure 1.1 FTICR-MS.....	4
Figure 1.2 A cubic analyzer cell in FTMS.....	4
Figure 1.3 Electrospray ionization.....	5
Figure 1.4 Schematic of a 3D ion trap mass spectrometer	6
Figure 1.5 Schematic of a 2D linear ion trap mass spectrometer	6
Figure 1.6 Schematic of FT-ICR dual cell bracketing experiments	7
Figure 1.7 Schematic of LCQ bracketing experiments.....	8
Figure 1.8. CID of proton-bound complex of acid and reference acid	9
Figure 2.1 Electron delocalization of N1-deprotonated uracil.....	11
Figure 2.2 Transition state of S_N2 reaction between 3-methyl uracil and formate.....	12
Figure 2.3. Bracketing method for acidity measurement.....	14
Figure 2.4 Bracketing method for S_N2 reaction.....	15
Figure 2.5 Substituted aniline compounds and substituted amine compounds	16
Figure 2.6 The distances between N-C (r_1) and C-O (r_2) in the transition state	21
Figure 2.7 Transition state of thermoneutral reaction of HCOO^- and HCOOCH_3	21
Figure 2.8 The distances between N-C (r_1) and C-Cl (r_2) in the transition state	23
Figure 2.9 Transition state of thermoneutral reaction of Cl^- and CH_3Cl	23

Figure 2.10 Schematic of S_N2 reaction between nucleophiles and tert-butyl methyl(phenyl)carbamate	27
Figure 2.11 Schematic of S_N2 reaction between nucleophiles and N, N-dimethylacrylamide.....	28
Figure 3.1. Pd-NHC-complexes for the Mizoroki-Heck reaction.....	32
Figure 3.2. Tunable aryl-alkyl ionic liquid (TAAILs)	32
Figure 3.3 Interrelationship between the gas phase and solution thermodynamic parameters	34
Figure 4.1 Structures of Grubbs catalysts	49
Figure 4.2 Elimination and substitution pathway for di-methylimidazolium*phosphine dimer	50
Figure 4.3 Elimination and substitution pathway for di- CD_3 -imidazolium*phosphine dimer	51
Figure 4.4 Di- CD_3 -imidazolium*phosphine dimer.....	52
Figure 4.5 Oxidation of phosphine	52
Figure 4.6 Substitution pathway for di- CD_3 -imidazolium*phosphine dimer	53

LIST OF TABLES

Table 2.1. ΔH_{acid} , ΔH^\ddagger and $\Delta\Delta H^\ddagger/\Delta\Delta H_{\text{acid}}$ of substituted aniline compounds	18
Table 2.2. ΔH_{acid} , ΔH^\ddagger and $\Delta\Delta H^\ddagger/\Delta\Delta H_{\text{acid}}$ of substituted amine compounds.....	20
Table 2.3. ΔH_r , r_1 , r_2 , and ratio of $(1.97653-r_2)/1.97653$ of S_N2 reaction between formate and electrophiles with different substitutes for amine system.....	22
Table 2.4 ΔH_r , r_1 , r_2 , and ratio of $(2.37126-r_2)/2.37126$ of S_N2 reaction between chloride and electrophiles with different leaving groups for amine system	24
Table 2.5 Summary of results for acidity bracketing of more acidic site of tert-butyl phenylcarbamate	24
Table 2.6 Summary of results for acidity bracketing of more acidic site of methyl phenylcarbamate	25
Table 2.7 Summary of results for acidity bracketing of more acidic site of acrylamide ...	26
Table 2.8 S_N2 reaction between nucleophiles and tert-butyl methyl(phenyl)carbamate ...	28
Table 2.9 S_N2 reaction between nucleophiles and N, N-dimethylacrylamide	29
Table 3.1. Calculated gas-phase deprotonation energies (PA), solvation energies, and experimental and calculated pK _a values for imidazolium-like compounds in DMSO	35
Table 3.2. Calculated gas-phase deprotonation energies (PA), solvation energies, and experimental and calculated pK _a values for imidazolium-like compounds in H ₂ O	38
Table 3.3 Calculated pK _a of Stassner's carbenes by applying Bartberger's method.....	40
Table 3.4 Calculated gas phase proton affinity (PA), solvation free energies of ionization (ΔG_a), and experimental and calculated pK _a values in DMSO	40

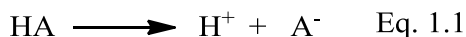
Table 3.5 Calculated gas phase proton affinity (PA), solvation free energies of ionization (ΔG_a), and experimental and calculated pK_a values in H_2O	43
Table 3.6 Calculated pK_a of Stassner's carbenes by applying Ogretir's method	45
Table 3.7 Summary of proton affinity of 1-(4-methoxyphenyl)-3-methyl-1H-imidazol-3-ium	45
Table 3.8 Summary of proton affinity of 3-methyl-1-phenyl-1H-imidazol-3-ium.....	46
Table 3.9 Summary of proton affinity of 1-(4-bromophenyl)-3-methyl-1H-imidazol-3-ium	46
Table 3.10 Calculated pK_a of Stassner's carbenes by applying Method 1-3	47

Chapter 1 Introduction

1.1 Overview

1.1.1 Gas phase acidity and proton affinity

The gas phase provides a valuable environment to examine the intrinsic properties and reactivity of organic molecules.¹ We can exclude the solvation effect in solution phase by studying the gas phase properties, and giving better understanding of the intrinsic properties of molecules. The gas phase acidity is defined as the positive enthalpy change (ΔH_{acid}) of the deprotonation reaction (Eq. 1.1), ranging from 314 to 417 kcal/mol. The gas phase proton affinity (PA) is defined as the negative enthalpy change of the protonation reaction, ranging from 130 to 291 kcal/mol² (Eq. 1.2). The lower value of gas phase acidity corresponding to higher acidity, while the higher value of proton affinity corresponding to a higher basicity.



In previous work, we have reported the gas phase thermochemical properties of uracil and 3-methyl uracil^{3,4}. Our studies are motivated by understanding how the acidity of conjugate acid relates with the leaving group ability in S_N2 reaction. In Chapter 2, we will describe the gas phase acidity and reactivity studies of a series of organic compounds with different substituent. In Chapter 3 and 4, we will focus on N-heterocyclic carbenes (NHCs) by measuring the proton affinity and probe the reactivity of proton-bounded dimer.

1.1.2 Gas phase thermochemical property study of substituted aniline and amine

In the gas phase, leaving group ability is known to be better with higher acidity (lower ΔH_{acid}) of the conjugate acid. However, the leaving group ability of 3-methyl uracil anion is different from chloride even though 3-methyl uracil and hydrochloride have similar gas phase acidity⁵. Aniline has a structure that is similar as uracil, and easily to functionalize and access commercially. Therefore, we chose aniline with different substituent to probe the problem. However, we did not get the result as we expected and the reason is that the electron delocalization ability of aromatic ring in aniline minimized the difference between different substituent. Thus we designed the substituted amine instead to examine the relation between leaving group ability and acidity and proved our hypothesis.

1.1.3 Gas phase proton affinity of N-heterocyclic carbenes (NHCs)

N-heterocyclic carbenes are ligands of a variety of organometallic catalysts and demonstrated broad applications in organic synthesis^{6,7,8,9}, such as olefin metathesis and Mizoroki-Heck coupling. The protonated NHCs are ionic liquids, and can be used as green solvent in organic synthesis¹⁰. The thermochemical properties of these carbenes and ionic liquids are barely known, especially the gas phase proton affinity and acidity. We are interested in the proton affinity of NHCs (acidity of imidazolium cations) and trying to find the relation between proton affinity and catalytic ability.

1.2 Instrumentation

1.2.1 FTMS

The Fourier transform ion cyclotron resonance mass spectrometer (FT-ICR) is a highly accurate mass analyzer that detects ions by mass to charge ratio (m/z)^{11,12}. The basic principle for the mass analyzer is to detect ions based on the relation between m/z and cyclotron frequency (ω) (Eq. 1.3). It shows that the m/z ratio only depends on the cyclotron frequency and magnetic strength¹³.

$$\omega = \frac{eB}{m}, e=\text{Faraday constant}, B=\text{magnetic field strength}, \quad \text{Eq. 1.3}$$

For S_N2 reaction and acidity measurement, a Finnigan 2001 FT-ICR with a dual cell setup (Figure 1.1) was used. Both cells (Figure 1.2) are composed of three pairs of plates: the trapping plates that have a hole in the center to allow ions or electrons to enter, the detection plates and excitation plates. The ions are excited to a higher orbit by the swept radio frequency pulse on the two excitation plates, and their motions will induce an alternating current (image current) between the detection plates, which is amplified, quantified and transformed into frequency domain signals.

Gas phase reactions were carried out in a two collinearly adjacent 1 inch cubic cells, that is surrounded by 3.3 T magnetic field, which is generated by a superconducting magnetic. By changing the voltage of the parallel plates, ions can be transferred from either the left cell (source cell) to the right cell (analyzer cell) or in the opposite direction and then be cooled by argon which is pulsed in via pulsed valves. The pressure of the dual cell needs to be kept at around 10^{-9} torr.

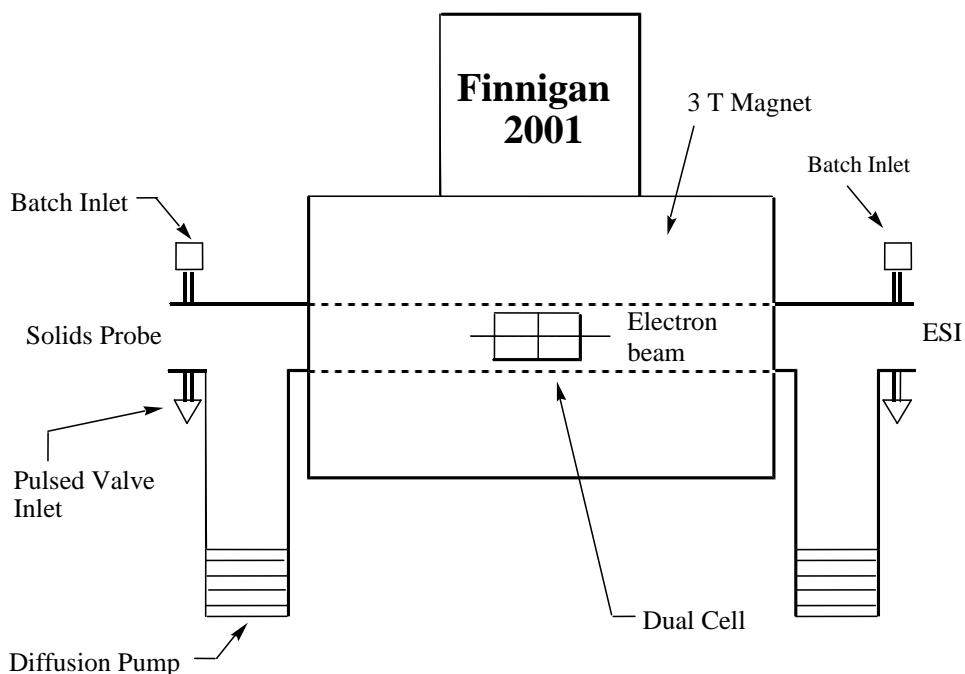


Figure 1.1 FTICR-MS

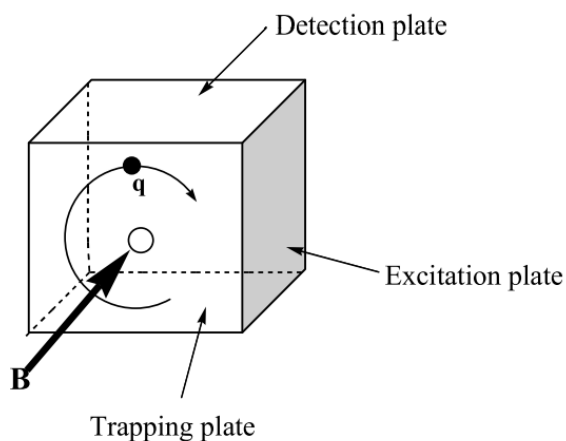


Figure 1.2 A cubic analyzer cell in FTMS

1.2.2 ESI and ion trap mass spectrometer

Electrospray ionization (ESI) is a technique that is called "soft" ionization, which ionizes the sample at atmospheric pressure by applying a strong electric field (3-6kV) at the capillary tip and typically does not produce fragmentation.¹⁴ The samples are dissolved in a polar solvent (water, methanol or acetonitrile, etc) and injected into the mass spectrometer at a flow rate of 1 $\mu\text{L}/\text{min}$ to 1 mL/min . The process of ESI is illustrated in Figure 1.3.

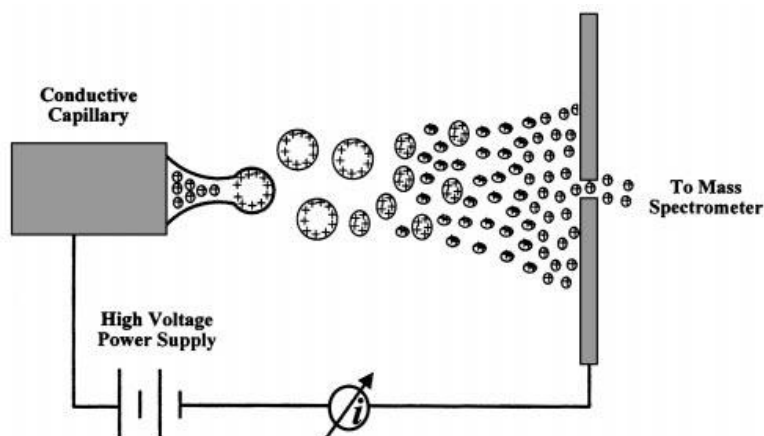


Figure 1.3 Electrospray ionization

The quadrupole ion trap is a highly sensitive and specific mass spectrometer that consists of one ring electrodes and two endcap electrodes¹⁵ (Figure 1.4). Ions are generated by ESI and then trapped, excited and ejected by the three hyperbolic electrodes cavity. AC and DC are applied on the electrodes and damping gas (helium, 1m Torr) is filled in the ion trap. The ions move toward the center of ion trap, destabilize and eject by altering the amplitude of the AC.

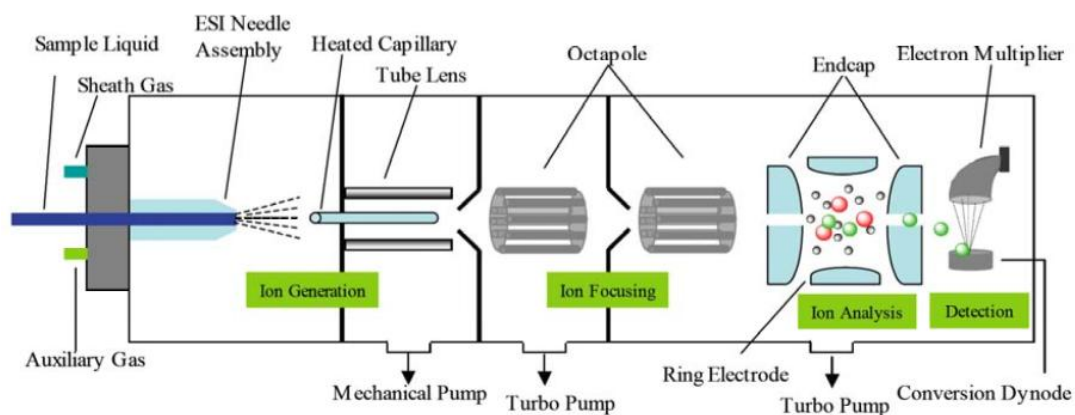


Figure 1.4 Schematic of a 3D ion trap mass spectrometer

The linear ion trap is another type of mass spectrometer, which contains a square array of hyperbolic electrodes¹⁶ (Figure 1.5). Ions enter into the center of ion trap, and then accelerate and move into the linear ion trap by applying a RF voltage and DC potentials on the electrodes. Linear ion trap has higher sensitivity and larger ion storage capacity compared to quadropole ion trap.

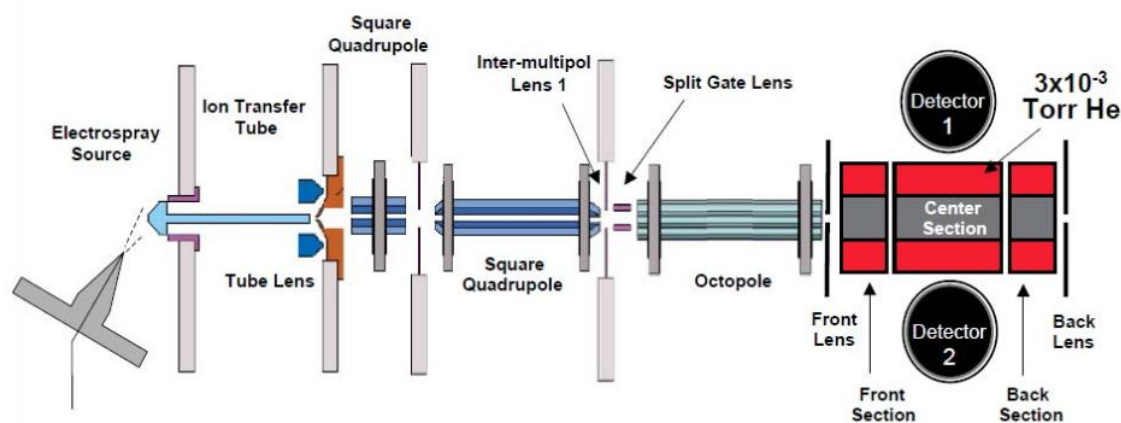


Figure 1.5 Schematic of a 2D linear ion trap mass spectrometer

1.3 Methodology

1.3.1 Bracketing method in FTMS

We use the bracketing method to measure the gas phase acidity and proton affinity of compounds. We choose reference acids/bases with known acidity/ proton affinity to examine the acidity/ proton affinity of unknown compound by the occurrence/non-occurrence of a proton transfer reaction^{iii,iv} (Figure 1.6).

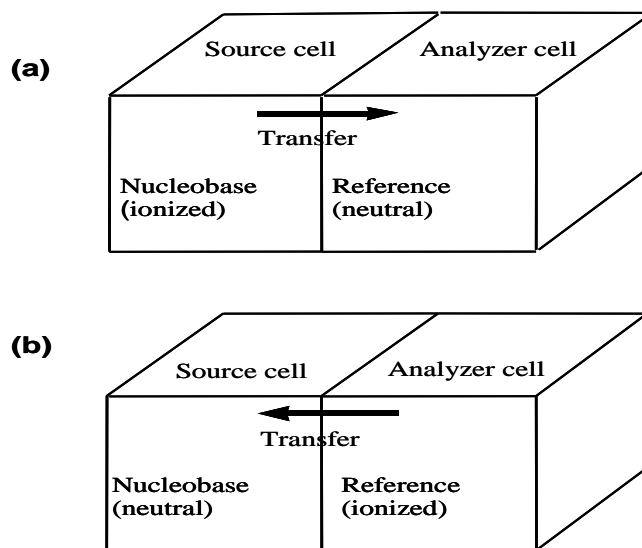


Figure 1.6 Schematic of FT-ICR dual cell bracketing experiments

For acidity experiments, deprotonated sample compounds are generated in the source cell by chemical ionization with hydroxide anion and then transferred to the analyzer cell to react with the neutral reference acids. Meanwhile, the deprotonated reference acid could also be transferred to source cell react with neutral sample compounds. The acidity of unknown acid can be measured by comparing with a series of reference acid by monitoring proton transfer reactions.

For S_N2 reaction, a series of nucleophiles with different proton affinities are chosen to react with the organic species we are studying. The nucleophiles are generated from the deprotonation of commercially available neutral reference acids, and transferred from analyzer cell to source cell, reacting with neutral organic compounds. Efficiencies of S_N2 reaction are determined by the proton affinity of nucleophiles: the nucleophiles are chosen to have a PA as high as possible, but lower than the most acidic site of studied compound to prevent protonation reaction. By monitoring the m/z of newly generated ions, the products from the reaction between sample compounds and nucleophiles can be determined.

1.3.2 Bracketing method in LCQ

Reference base is introduced into LCQ by vaporizing as neutral compound. The studied compound is dissolved in the solvent ($<100\mu\text{M}$) and isolated as protonated compound to react with neutral reference at different reaction time from 0.03ms to more than 1000ms. The proton affinity of studied compound is determined by the protonation reaction between compound anions and neutral reference. If protonation occurs, PA of compound is higher than reference; while if there is no protonation reaction, PA is lower than reference. The setup of LCQ bracketing method is illustrated in Figure 1.7.

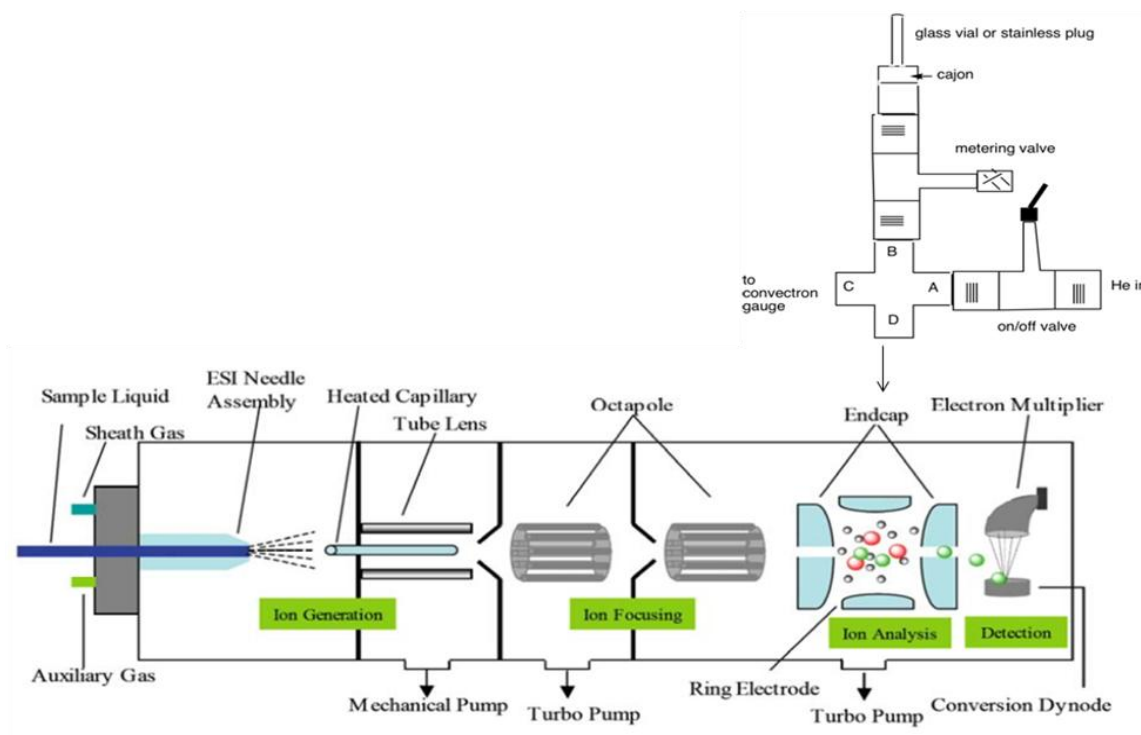


Figure 1.7 Schematic of LCQ bracketing experiments

1.3.3 Cooks Kinetic Method

The Cooks Kinetic Method was developed by Cooks and coworkers in the 1970s^{17,18,19,20}. This approach uses kinetic information to study the thermochemical properties in the gas phase. Cooks kinetic methods involves two competitive reactions (Figure 1.8):

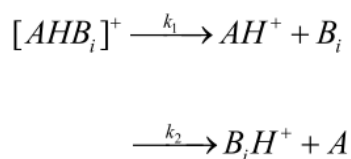
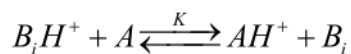


Figure 1.8. CID of proton-bound complex of acid and reference acid

AH^+ represents the compound with unknown acidity and B_iH^+ represents a series of reference acids. In our experiments, the Cooks Kinetic Method was performed in a quadrupole ion trap mass spectrometer (Thermo Finnigan LCQ). sample compound are mixed with reference acids in methanol. The mixed solutions were ionized by electrospray ionization (ESI) and the proton-bound complex ions (dimers) were isolated and subjected to collision-induced dissociation (CID) in the ion trap analyzer.

Data were analyzed by both standard Cooks Kinetic Method. The ratio of rate constants (k_1/k_2) of the two dissociation pathways is represented by the ratio of relative ion abundance of the A⁺/Ref⁺. Acidity of sample compound relative to the reference acids are calculated by Eq. 1.4. $\ln(k_1/k_2)$ was plotted versus the known acidity for a series of references, and the acidity of sample compounds can be obtained directly from the intercept of the resulting line.



$$K \approx k_1 / k_2$$

$$PA(A) - PA(B_i) \approx RT_{eff} \ln K$$

$$\ln(k_1 / k_2) = \frac{1}{RT_{eff}} (PA(A) - PA(B_i)) \quad \text{Eq. 1.4}$$

1.3.4 Calculations

Relative energies (gas phase acidities and proton affinities) of all compounds that we studied were calculated using the B3LYP method with 6-31+G* basis set in Gaussian 03²¹, and all the geometries are fully optimized at 298K. Solvation studies are conducted using the conductor-like polarizable continuum model (CPCM), where molecules are optimized at B3LYP/6-31+G* and UAKS radii are used^{22,23}. A dielectric constant of 78.4 is used to simulate an aqueous environment.

Chapter 2 S_N2 project

2.1 Introduction

Uracil is a nucleobase which can arise from DNA by cytosine deamination and also be misincorporated into DNA^{24,25,26}. The enzyme uracil DNA glycosylase (UDG) removes uracil from the genome and the mechanism involves *N*-deprotonated uracil as a leaving group^{27,28}.

In general, the acid strength of an acid is related to the leaving group ability of its conjugate base. However, the studies we did previously showed that 3-methyluracil is as acidic as hydrochloric acid in the gas phase, while the leaving group abilities of their deprotonated 3-methyluracil and chloride are different. Chloride is a slightly better leaving group than deprotonated 3-methyluracil. To explain this result, we proposed that the reason why 3-methyluracil is very acidic is due to electron delocalization (Figure 2.1), which cannot be not fully recognized in the transition state of S_N2 reaction (Figure 2.2).

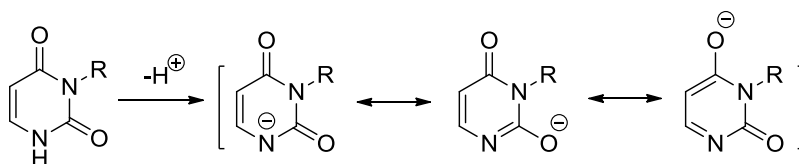


Figure 2.1 Electron delocalization of N1-deprotonated uracil

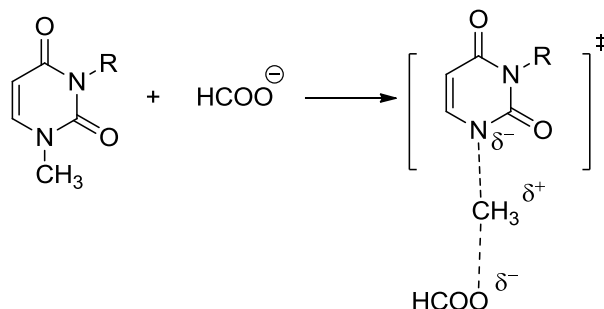


Figure 2.2 Transition state of S_N2 reaction between 3-methyl uracil and formate

Therefore, we designed a system with a series of electrophiles with different leaving groups to test our hypothesis. The leaving groups were chosen based on whether they could delocalize electrons or not. The groups with the ability to delocalize electrons are called “resonance stabilized groups”, while the others are called “non-resonance stabilized groups”. We are expecting a better correlation of acidity and leaving group ability for the non-resonance stabilized anion than the resonance stabilized anions.

In addition to study the relationship between acidity and leaving group ability, which is the initial motivation for the study we also test the Hammond postulate based on the data we collected from the calculation. The study we did showed that the transition state become early when the reaction is more exothermic, which agrees with Hammond postulate. The electrophiles with resonance stabilized substitutes have an earlier transition state than non-resonance stabilized one.

2.2 Experimental

All chemicals are commercially available except for tert-butyl methyl(phenyl)carbamate, which was synthesized following literature procedure²⁹. Gas

phase acidities of *N*-Boc aniline, methyl phenylcarbamate and acrylamide were measured by bracketing method with the Fourier transform ion cyclotron resonance mass spectrometer (FT-ICR), which is also known as Fourier Transform Mass Spectrometer (FTMS). S_N2 reactions of tert-butyl methyl(phenyl)carbamate and *N*, *N*-dimethylacryamide were conducted with FT-ICR as well. Gas phase calculations of the acidity and enthalpy of transition state were conducted for reference and guidance of experiments.

For the acidity measurement, *N*-Boc aniline, methyl phenylcarbamate and acrylamide were introduced into the source cell via solid probe without heating up. For the S_N2 reaction, tert-butyl methyl(phenyl)carbamate and *N*, *N*-dimethylacryamide were introduced into the source via batch inlets without heating up. Reference acids were introduced via analyzer batch inlets, pulsed valves with or without heating. All reactions were conducted at room temperature.

By applying bracketing method, a series of compounds with known acidity were used as references. For acidity experiments, deprotonated *N*-Boc aniline, methyl phenylcarbamate and acrylamide were generated in the source cell by chemical ionization with OH^- ion and then transferred to the analyzer cell to react with the neutral reference acids (Figure 2.3 a). Meanwhile, the deprotonated reference acid could also be transferred to source cell react with neutral *N*-Boc aniline, methyl phenylcarbamate and acrylamide (Figure 2.3 b). The acidity of unknown acid can be measured by comparing with a series of reference acid by monitoring the occurrence of proton transfer reactions.

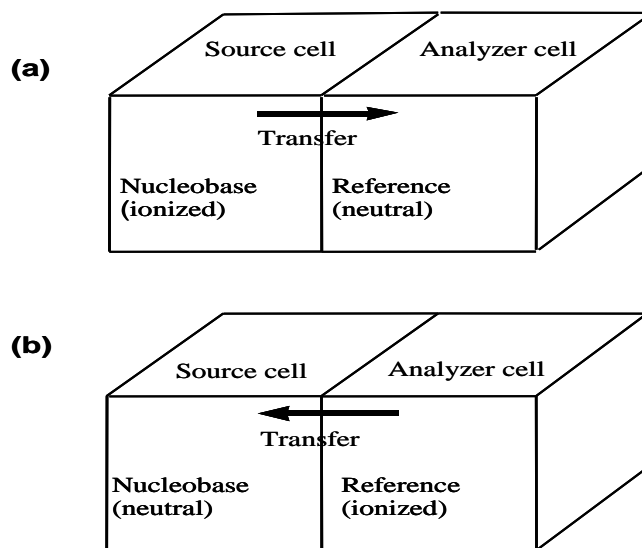


Figure 2.3. Bracketing method for acidity measurement

For S_N2 reaction, a series of nucleophiles was chosen to react with *tert*-butyl methyl(phenyl)carbamate and *N, N*-dimethylacryamide. The nucleophiles were generated from commercially available neutral reference acids, deprotonated by hydroxide ions and transferred from analyzer cell to source cell, reacting with neutral *tert*-butyl methyl(phenyl)carbamate and *N, N*-dimethylacryamide. By monitoring the m/z of newly generated ions, the products from the reaction between *tert*-butyl methyl(phenyl)carbamate and *N, N*-dimethylacryamide and nucleophiles can be determined (Figure 2.4)

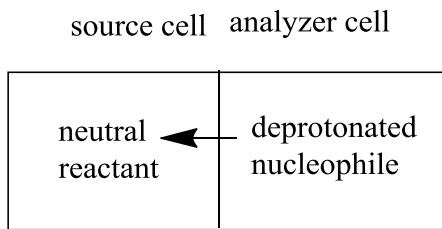


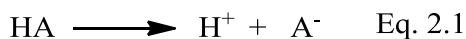
Figure 2.4 Bracketing method for S_N2 reaction

Relative energies of a series of substituted aniline compounds and substituted amine were calculated using the B3LYP method with 6-31+G* basis set in Gaussian 03. All the gas phase acidities were calculated at B3LYP/6-31+G* level as well, and all the geometries are fully optimized at 298K.

2.3 Results

2.3.1 Computational results: acidities, ΔH^\ddagger

Substituted aniline and substituted amine systems were chosen because they resemble to uracil and easy to functionalize. Both resonance stabilized groups and non-resonance stabilized groups are chosen (Figure 2.5). When X=resonance stabilized groups, Z=H; while when X= non-resonance stabilized groups, Z=the same groups or H. We used Y=H to calculate the acidity (ΔH_{acid}), and Y=CH₃ to calculate the ΔH^\ddagger for S_N2 reaction (nucleophile is formate). The gas phase acidity (ΔH_{acid}) is defined as the positive enthalpy change associated with the deprotonation of HA to form H⁺ and A⁻ (Eq. 2.1). The leaving group ability is represented by the enthalpy changes of the corresponding transition state (ΔH^\ddagger) of S_N2 reaction between formate and substituted aniline or amine.



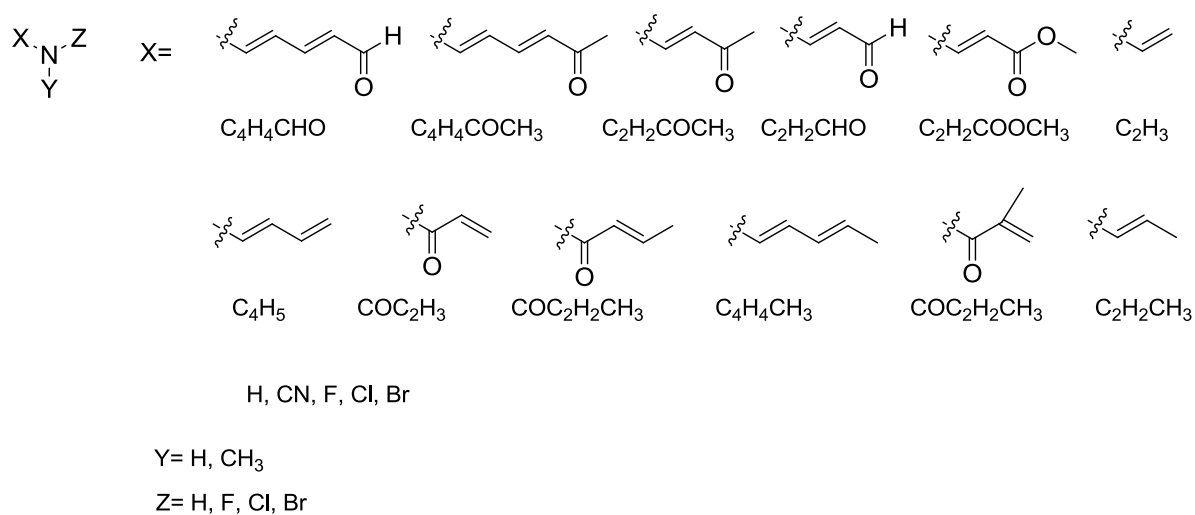
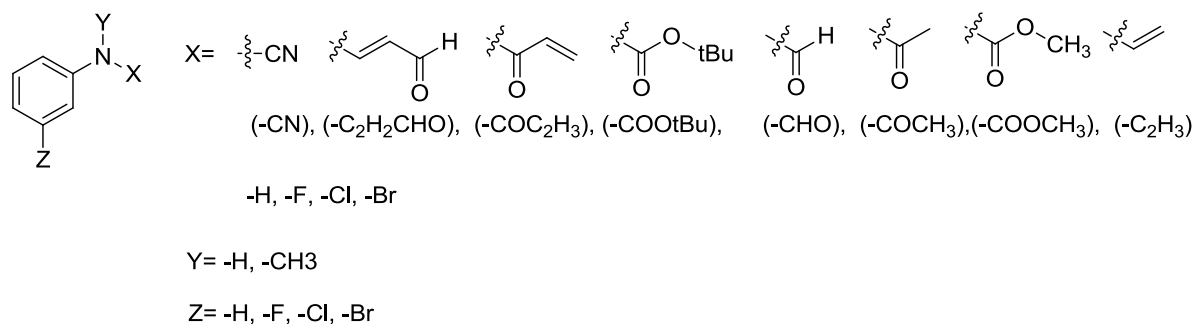


Figure 2.5 Substituted aniline compounds and substituted amine compounds

$\Delta\Delta H^\ddagger$ of substituted aniline compounds is defined as the difference of ΔH^\ddagger between the different substituted aniline compounds and aniline ($X=Y=Z=H$); and $\Delta\Delta H^\ddagger$ of substituted amine compounds is defined as the difference of ΔH^\ddagger between the different substituted amine compounds and ammonia ($X=Y=Z=H$). The results of ΔH_{acid} , ΔH^\ddagger and $\Delta\Delta H^\ddagger$ of substituted aniline are listed in Table 2.1, and the results of ΔH_{acid} , ΔH^\ddagger and $\Delta\Delta H^\ddagger$ of substituted amine are listed in Table 2.2.

Substituent X	Substituent Z	ΔH_{acid} , kcal/mol	ΔH^\ddagger , kcal/mol	$\Delta\Delta H^\ddagger/\Delta\Delta H_{\text{acid}}$
H	H	365.30(0)	32.84(0)	-
C ₂ H ₂ CHO	H	334.00(31.30)	11.43(21.41)	0.68
COC ₂ H ₃	H	346.07(19.23)	19.10(13.74)	0.71
COO ^t Bu	H	346.90(18.40)	21.26(11.58)	0.63
CHO	H	348.60(16.70)	17.93(14.91)	0.89
COCH ₃	H	348.56(16.74)	22.34(10.50)	0.63
COOCH ₃	H	349.20(16.10)	16.31(16.53)	1.03
C ₂ H ₃	H	351.90(13.40)	25.22(7.62)	0.57
CN	H	327.46(37.84)	8.61(24.23)	0.64
F	H	343.31(21.99)	20.27(12.57)	0.57
F	F	337.28(28.02)	15.23(17.61)	0.63
H	F	359.47(5.83)	27.67(5.17)	0.89
Cl	H	344.40(20.58)	5.12(27.72)	1.33
Cl	Cl	335.72(29.58)	12.77(20.07)	0.68
H	Cl	357.51(7.79)	26.23(6.61)	0.85
Br	H	358.13(7.17)	18.61(14.23)	1.98
Br	Br	398.72(33.42)	42.44(9.60)	0.29
H	Br	356.93(8.37)	26.57(6.27)	0.75

Table 2.1. ΔH_{acid} , ΔH^\ddagger and $\Delta\Delta H^\ddagger/\Delta\Delta H_{\text{acid}}$ of substituted aniline compounds

Substituent X	Substituent Z	ΔH_{acid} , kcal/mol	ΔH^\ddagger , kcal/mol	$\Delta\Delta H^\ddagger/\Delta\Delta H_{\text{acid}}$
H	H	399.50(0)	52.88(0)	-
C ₄ H ₄ CHO	H	342.99(56.51)	13.65(39.23)	0.69
C ₄ H ₄ COCH ₃	H	344.71(54.79)	17.85(35.03)	0.64
C ₂ H ₂ COCH ₃	H	348.17(51.33)	21.11(31.77)	0.62
C ₂ H ₂ CHO	H	351.60(47.90)	21.93(30.95)	0.65
C ₂ H ₂ COOCH ₃	H	354.85(44.65)	25.49(27.39)	0.61
C ₂ H ₃	H	373.81(25.69)	36.99(15.89)	0.62
C ₂ H ₃	C ₂ H ₃	354.80 (44.70)	27.45(25.43)	0.57
C ₄ H ₅	H	356.81(42.69)	25.22(27.66)	0.65

COC_2H_3	H	355.46(44.04)	27.94(24.94)	0.57
$\text{COC}_2\text{H}_2\text{CH}_3$	H	359.20(40.30)	30.54(22.34)	0.55
$\text{C}_4\text{H}_4\text{CH}_3$	H	364.68(34.82)	30.55(22.33)	0.64
$\text{COC}_2\text{H}_2\text{CH}_3$	H	373.73(25.77)	34.45(18.43)	0.72
$\text{C}_2\text{H}_2\text{CH}_3$	H	374.67(24.83)	35.48(17.40)	0.70
CN	CH	345.22(54.28)	15.51(37.37)	0.69
F	H	378.72(20.78)	39.68(13.20)	0.64
F	F	356.03(43.47)	23.55(29.33)	0.67
Cl	H	372.66(26.84)	32.84(20.04)	0.75
Cl	Cl	346.26(53.24)	15.17(37.71)	0.71
Br	H	370.32(29.18)	31.20(21.68)	0.75
Br	Br	344.75(54.75)	13.24(39.64)	0.72

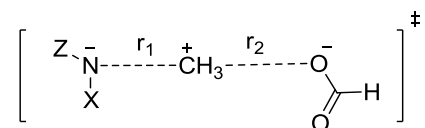
)	
--	--	--	---	--

Table 2.2. ΔH_{acid} , ΔH^\ddagger and $\Delta\Delta H^\ddagger/\Delta\Delta H_{\text{acid}}$ of substituted amine compounds

2.3.2 Computational results: r_1 , r_2

Hammond postulate states that the transition state becomes earlier when the reaction is more exothermic. The distances between N-C (r_1) and C-O (r_2) in the transition state (Figure 2.6) and the enthalpy of the S_N2 reaction (ΔH_r) with formate as nucleophile (Eq. 2.2) were calculated to test the Hammond postulate.

The distance between C-O for the thermoneutral reaction of HCOO^- and HCOOCH_3 was calculated to be 1.97653 Å (Figure 2.7). The ratio of $(1.97653 - r_2)/1.97653$ is used to determine if the transition state is early or late for S_N2 reaction with formate. The larger the number of the ratio is, the later the transition state will be. ΔH_r , r_1 , r_2 , and ratio of $(1.97653 - r_2)/1.97653$ of S_N2 reaction between formate and different substituted amine are listed in Table 2.3.



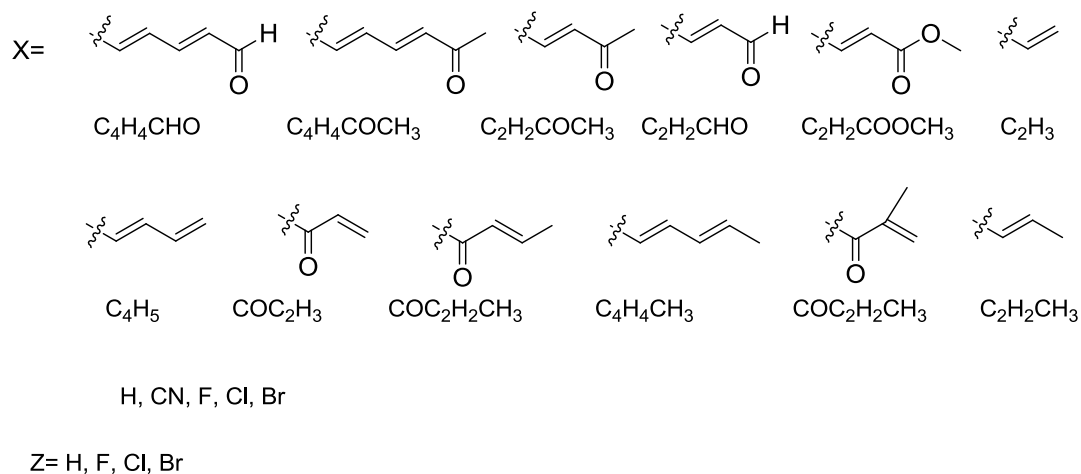


Figure 2.6 The distances between N-C (r_1) and C-O (r_2) in the transition state

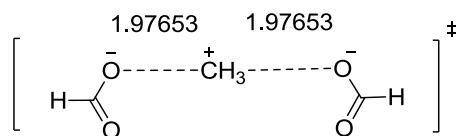


Figure 2.7 Transition state of thermoneutral reaction of $HCOO^-$ and $HCOOCH_3$

Substituent X	Substituent Z	ΔH_r , kcal/mol	r_1	r_2	$(1.97653 - r_2)/1.97653$
C_4H_4CHO	H	4.9	2.069	1.898	0.0399
$C_4H_4COCH_3$	H	7.2	2.039	1.887	0.0451
$C_2H_2COCH_3$	H	12.2	2.064	1.873	0.0525
C_2H_2CHO	H	15.1	2.100	1.870	0.0538
$C_2H_2COOCH_3$	H	17.7	2.086	1.854	0.0622
C_2H_3	H	20.1	2.204	1.822	0.0780

C ₂ H ₃	C ₂ H ₃	19.2	2.085	1.889	0.0441
C ₄ H ₅	H	24.3	2.135	1.851	0.0636
COC ₂ H ₃	H	20.3	2.121	1.873	0.0523
COC ₂ H ₂ CH ₃	H	22.2	2.095	1.873	0.0526
C ₄ H ₄ CH ₃	H	26.7	2.130	1.837	0.0707
C ₂ H ₂ CH ₃	H	37.6	2.217	1.827	0.0756
H	H	64.0	2.425	1.697	0.1420
CN	H	9.17	2.085	1.890	0.0438
F	H	48.0	2.338	1.720	0.1296
F	F	28.4	2.216	1.770	0.1046
Cl	H	38.6	2.268	1.756	0.1118
Cl	Cl	12.6	2.120	1.849	0.0644
Br	H	36.8	2.246	1.767	0.1061
Br	Br	13.4	2.091	1.871	0.0532

Table 2.3. ΔH_r , r_1 , r_2 , and ratio of $(1.97653-r_2)/1.97653$ of S_N2 reaction between formate and electrophiles with different substitutes for amine system

Chloride was chosen as a weak nucleophile corresponding to a slow reaction. The distances between N-C (r_1) and C-Cl (r_2) in the transition state (Figure 2.8) and the enthalpy of the S_N2 reaction (ΔH_r) (Eq. 2.3) with chloride as nucleophile were calculated, and the distances between C-Cl for the thermoneutral reaction of Cl^- and CH_3Cl was calculated to be 2.37126 Å (Figure 2.9) at B3LYP/6-31+G* level. The ratio of $(2.37126-r_2)/2.37126$ was used to determine if the transition state is early or late for S_N2 reaction with chloride. ΔH_r , r_1 , r_2 , and ratio of $(2.37126-r_2)/2.37126$ of S_N2 reaction between chloride and substituted amine are listed in Table 2.4.

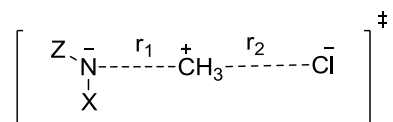
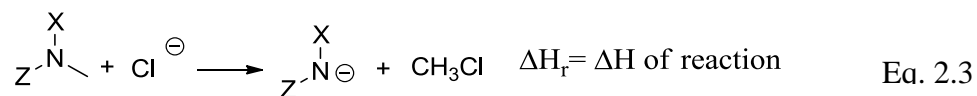


Figure 2.8 The distances between N-C (r_1) and C-Cl (r_2) in the transition state

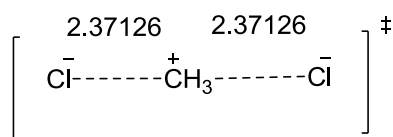


Figure 2.9 Transition state of thermoneutral reaction of Cl^- and CH_3Cl

Substituent X	Substituent Z	ΔH_r , kcal/mol	r_1	r_2	$(2.37126 - r_2)/2.37126$
$\text{C}_4\text{H}_4\text{CHO}$	H	14.4	2.133	2.242	0.0545
$\text{C}_4\text{H}_4\text{COCH}_3$	H	16.7	2.138	2.239	0.0604
$\text{C}_2\text{H}_2\text{COCH}_3$	H	21.7	2.173	2.218	0.0815
$\text{C}_2\text{H}_2\text{CHO}$	H	24.6	2.199	2.199	0.0936
$\text{C}_2\text{H}_2\text{COOCH}_3$	H	27.2	2.207	2.193	0.1047
C_2H_3	H	29.6	2.335	2.131	0.1148
C_2H_3	C_2H_3	28.7	2.197	2.228	0.1111
C_4H_5	H	33.8	2.252	2.178	0.1325
COC_2H_3	H	29.8	2.218	2.202	0.1157
$\text{COC}_2\text{H}_2\text{CH}_3$	H	31.6	2.336	2.199	0.1234

C ₄ H ₄ CH ₃	H	36.2	2.271	2.170	0.1427
C ₂ H ₂ CH ₃	H	47.1	2.368	2.117	0.1885
CN	H	18.6	2.212	2.220	0.0686
F	F	37.8	2.444	2.046	0.1495
Cl	H	48.1	2.564	1.989	0.1928
Cl	Cl	22.1	2.235	2.165	0.0832
Br	H	46.3	2.489	2.024	0.1852
Br	Br	22.8	2.207	2.182	0.0862

Table 2.4 ΔH_r , r_1 , r_2 , and ratio of $(2.37126-r_2)/2.37126$ of S_N2 reaction between chloride and electrophiles with different leaving groups for amine system

2.3.3 Experimental results: acidities

The acidity of tert-butyl phenylcarbamate is measured to be 348.5 ± 3 kcal/mol (Table 2.5).

Table 2.5 Summary of results for acidity bracketing of more acidic site of tert-butyl phenylcarbamate

Reference compound	ΔH_{acid}^a	ΔG_{acid}^a	Proton transfer ^b	
			Ref. acid	Conj. base
Butyric acid	346.8 ± 2.1	339.5 ± 2.0	+	-
Acetic acid	347.4 ± 0.5	341.1 ± 2.0	+	-
Propanic acid	347.4 ± 2.2	340.4 ± 2.0	+	-
m-cresol	349.6 ± 2.1	342.7 ± 2.00	-	+

p-cresol	350.2 ± 2.2	343.4 ± 2.0	-	+
Pentane thiol	352.5 ± 2.3	346.2 ± 2.5	-	+

^a Acidities are in kcal mol⁻¹.⁸ ^bA “+” indicates the occurrence and a “-” indicates the absence of proton transfer.

The acidity of methyl phenylcarbamate is measured to be 348.5±3 kcal/mol (Table 2.6).

Table 2.6 Summary of results for acidity bracketing of more acidic site of methyl phenylcarbamate

Reference compound	ΔH_{acid}^a	ΔG_{acid}^a	Proton transfer ^b	
			Ref.	Conj.
			acid	base
2,4-pentanedione	343.8±2.1	336.7 ± 2.0	+	-
Butyric acid	346.8±2.1	339.5 ± 2.0	+	-
Acetic acid	347.4 ± 0.5	341.1 ± 2.0	+	-
m-cresol	349.6 ± 2.1	342.7 ± 2.0	-	+
pentanethiol	352.3±2.1	346.2 ± 2.5	-	+
propane-1-thiol	354.2±2.2	347.9 ± 2.0	-	+

^a Acidities are in kcal mol⁻¹.⁸ ^bA “+” indicates the occurrence and a “-” indicates the absence of proton transfer.

The acidity of acrylamide is measured to be 357.3 ± 3 kcal/mol (Table 2.7).

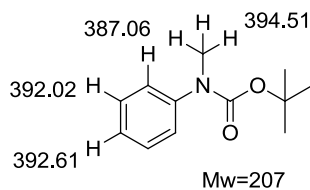
Table 2.7 Summary of results for acidity bracketing of more acidic site of acrylamide

Reference acid	ΔH_{acid}^a	ΔG_{acid}^a	Proton transfer ^b	
			Ref. acid	Conj. base
p-cresol	350.2 ± 2.2	343.4 ± 2.0	+	-
pentanethiol	352.5 ± 2.3	346.2 ± 2.5	+	-
4-(trifluoromethyl)-aniline	353.4 ± 2.1	346.0 ± 2.0	+	-
3-methylpyrazole	356.0 ± 2.1	348.3 ± 2.0	+	-
3-(trifluoromethyl)-aniline	356.9 ± 2.3	349.6 ± 2.0	+	-
Chloroacetonitrile	357.7 ± 2.1	350.0 ± 2.0	-	+
pyrrole	358.6 ± 2.1	350.9 ± 2.0	-	+

^a Acidities are in kcal mol⁻¹.⁸ ^b A “+” indicates the occurrence and a “-” indicates the absence of proton transfer.

2.3.4 Experimental results: S_N2 (tert-butyl methyl(phenyl)carbamate)

Nucleophiles were chosen based on: a. PA of nucleophiles should be high so as the nucleophilicity would be high. b. PA of nucleophiles cannot be higher than the most acidic part of tert-butyl methyl(phenyl) carbamate to prevent deprotonation, that is, PA should be < 387.06. ΔH_r , ΔG_r are calculated for S_N2 reaction and elimination reaction with formate as nucleophile (Figure 2.10). Reactions were allowed to go for up to 150 s. There was no S_N2 reaction occurred (Table 2.8).



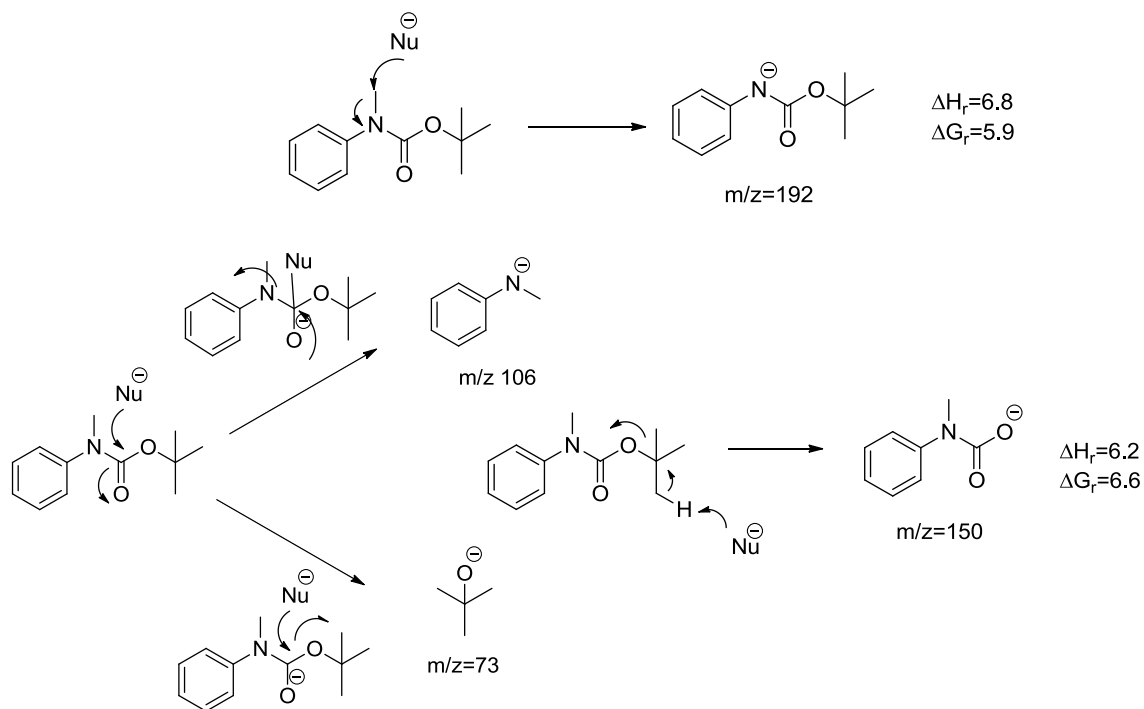
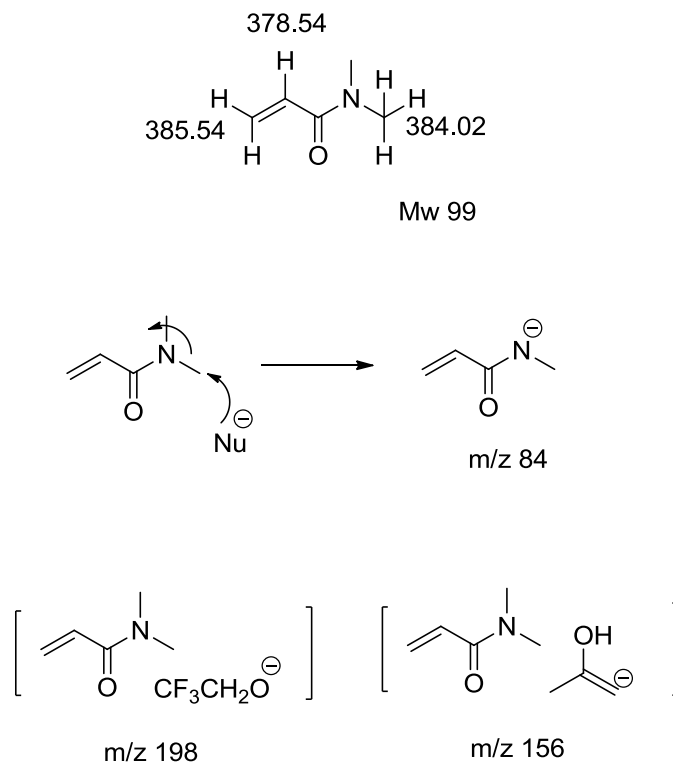


Figure 2.10 Schematic of S_N2 reaction between nucleophiles and tert-butyl methyl(phenyl)carbamate

Nucleophilic reagent	ΔH_{acid}	S_N2 reaction (m/z 192)
ethyl(phenyl)amide	364.1	-
phenylamide	366.4	-
2-methylpropan-2-olate	372.9	-
phenylmethanide	379.2	-
methanolate	382.0	-

Table 2.8 S_N2 reaction between nucleophiles and tert-butyl methyl(phenyl)carbamate2.3.5 Experimental results: S_N2 (N, N-dimethylacrylamide)

Nucleophiles were chosen based on: a. PA of nucleophiles should be high so as the nucleophilicity would be high. b. PA of nucleophiles cannot be higher than the most acidic part of N, N-dimethylacrylamide, that is, PA should be < 378.5 (Figure 2.11). There was no S_N2 reaction occurred (Table 2.9).

Figure 2.11 Schematic of S_N2 reaction between nucleophiles and N, N-dimethylacrylamide

nucleophilic reagent	ΔH_{acid}	S _N 2 reaction (m/z 84)
----------------------	--------------------------	------------------------------------

propane-1-thiolate	354.2	-
2,2,2-trifluoroethanolate	361.7	-
phenylamide	366.4	-
2-oxopropan-1-ide	366.4	-
2-methylpropan-2-olate	372.9	-

Table 2.9 S_N2 reaction between nucleophiles and N, N-dimethylacrylamide

2.4 Discussion & Conclusion

2.4.1 Relationship of leaving group ability and acidity

For substituted aniline, there is no difference between non-resonance stabilized and resonance stabilized groups in their leaving group ability tracking with acidity. The possible reason is that the benzene ring delocalizes the electron distribution, and therefore, reduce the difference between non-resonance stabilized and resonance stabilized groups.

For substituted amine, there is a slight difference between non-resonance stabilized and resonance stabilized in their leaving group ability correlate with acidity, which shows that the leaving group ability for non-resonance stabilized groups tracks better with acidity than resonance stabilized one. That is, anions can be stable conjugate base because of electron delocalization, but may not be a good leaving group because the delocalization cannot be fully recognized in S_N2 transition state.

2.4.2. Hammond postulate

The data also showed clearly that the transition state become early when the reaction is more exothermic, which agrees with Hammond postulate. In addition, the data shows that the electrophiles with resonance stabilized groups have an earlier transition state than those with non-resonance stabilized groups.

We would expect the weaker nucleophile chloride to generate later TS's than the same reaction with strong nucleophile formate. Therefore, we would expect that the reactions with chloride would allow less of a difference between resonance and non-resonance stabilized electrophiles. However, our results show a greater differentiation between resonance and non-resonance stabilized groups with chloride (versus formate). The resonance slope does not change with chloride versus formate; while the non-resonance slope does change – more sensitive with chloride .

Chapter 3 Strassner carbene project

3.1 Introduction

N-Heterocyclic singlet carbenes (NHCs), which were first isolated by Arduengo and coworkers in 1991, are of wide interest due to their variety application in synthesis, especially their catalytic applications^{30,31,32}. N-heterocyclic singlet carbenes (NHCs) are ligands of Pd-NHC-complexes catalyst for the Mizoroki-Heck coupling of aryl-halides with olefins (Figure 3.1). Strassner *et al.* stated that the stability and catalytic activity of *N*-aryl substituted Pt-complexes are higher than *N*-methyl substituted Pt-complexes, which could correlate to the difference in proton affinity between *N*-aryl substituted Pt-complexes and *N*-methyl substituted Pt-complexes. Therefore, it would be interesting to measure the proton affinity of *N*-aryl or *N*-alkyl substituted carbenes.

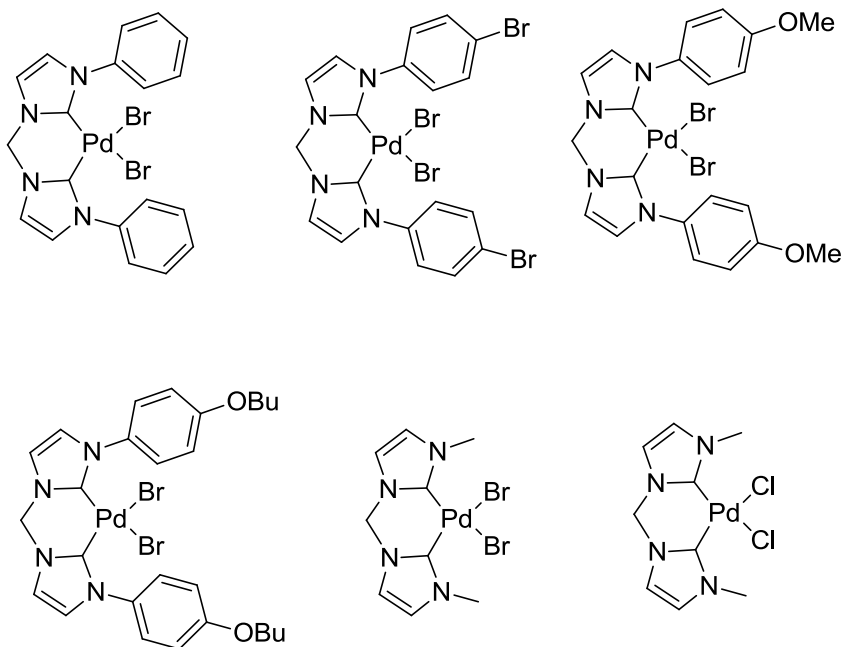


Figure 3.1. Pd-NHC-complexes for the Mizoroki-Heck reaction

In addition, imidazolium salts (protonated carbenes) is an important class of ionic liquid. They have been known as “green solvents” with several advantages over traditional organic solvents. Imidazolium could be used to design room-temperature ionic liquid but the properties of imidazolium-based salt are restricted by the alkyl chains on nitrogen.

To obtain a greater variation of ionic liquid properties, Strassner *et al.* designed a series of ionic liquids with the combination of sp^3 alkyl and sp^2 aryl substituent at the nitrogen of imidazolium core. The properties of this type aryl-alkyl ionic liquid are tunable by varying aryl substituent, so Strassner *et al.* termed it as tunable aryl-alkyl ionic liquid (TAAILs) (Figure 3.2).

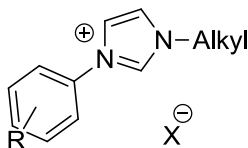


Figure 3.2. Tunable aryl-alkyl ionic liquid (TAAILs)

Strassner *et al* pointed out that the melting point of this new type of ionic liquid is tunable by changing the (para-) aryl substituent. However, no one has ever investigated the other fundamental properties of TAAILs. Therefore, we are interested in probing the acidities of TAAILs, which will aid people to understand and use this new type of ionic liquid better in the future.

3.2 Experimental

The structures are optimized at B3LYP/6-31+G* level and PA (calc, gas) are calculated on this level. The cpcm calculation is based on the optimized structure at B3LYP/6-31+G* scrf=(cpcm, read, solvent=water) and $\Delta\Delta G_{\text{solvation}}^\ddagger$ is obtained by cpcm calculation “total free energy in solution: with all non electrostatic terms”. The proton affinity (PA) are measured using bracekting method in LCQ. The pK_a are calculated based on Bartberger's method and Ogretir's method.

3.2.1 Bartberger's method

PA (calc, PCM) is obtained by $(\text{PA}_{\text{calc, gas}} - \Delta\Delta G_{\text{solvation}})$. PA (calc, PCM) vs pK_a (exp) was plotted in DMSO and equation $\text{PA}_{\text{(calc, PCM)}} = 0.3136 \text{ pK}_a (\text{in DMSO}) + 206.5$ was obtained.

3.2.2 Ogretir's method

The theoretical value of pK_a can be estimated from the thermodynamic cycle with Eq. 3.1. The Figure 3.3 gives the detailed explanation of the interrelationship between the gas phases and solution phases

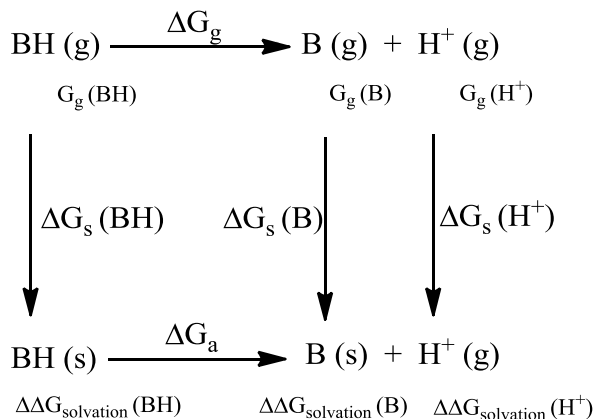


Figure 3.3 Interrelationship between the gas phase and solution thermodynamic parameters

$$\begin{aligned} \text{p}K_{\text{a}} &= \frac{\Delta G_{\text{a}}}{2.303RT} \\ &= \frac{[\Delta G_{\text{g}} + \Delta G_{\text{s}}(\text{B}) - \Delta G_{\text{s}}(\text{BH}) + \Delta G_{\text{s}}(\text{H}^+)]}{2.303RT} \end{aligned} \quad \text{Eq. 3.1}$$

ΔG_{g} is the gas phase free energies of ionization

ΔG_{a} is the solvation free energies of the ionization

ΔG_{s} 's are the solvation free energies of different species

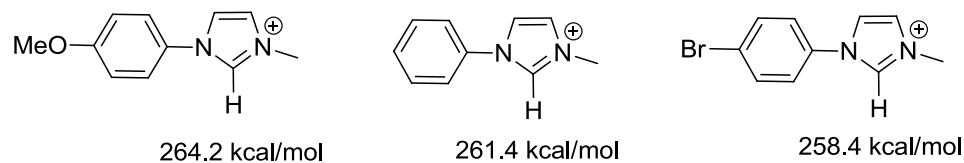
$\Delta G_{\text{s}}(\text{H}^+) = 259.5 \text{ kcal/mol}$

All geometry are optimized by HF/3-21G and reoptimized by B3LYP/6-31G*

The structures are optimized at B3LYP/6-31+G* level and G_{g} values (for BH, B and H^+) as well as PA (calc, gas) are calculated at this level. G_{g} is the “Sum of electronic and thermal Free Energies” of the molecules that obtained from the gauss output files. The single point CPCM calculation is based on the optimized structure by B3LYP/6-31+G* scrf=(cpcm, read, solvent=water) and ΔG_{s} values are obtained by subtracting G_{g} values from $\Delta\Delta G_{\text{solvation}}$ values (“total free energy in solution: with all non electrostatic terms” from CPCM calculation). ΔG_{a} values are obtained from equation 1 ($\Delta G_{\text{a}} = \Delta G_{\text{g}} + \Delta G_{\text{s}}(\text{B}) - \Delta G_{\text{s}}(\text{BH}) + \Delta G_{\text{s}}(\text{H}^+)$). $\text{p}K_{\text{a}}$ (calc) is obtained by $(\Delta G_{\text{a}})/1.36$. $\text{p}K_{\text{a}}$ (exp) vs $\text{p}K_{\text{a}}$ (calc) was plotted.

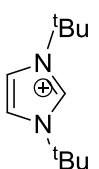
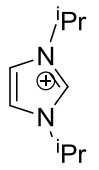
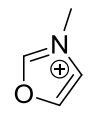
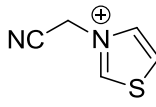
3.3 Results

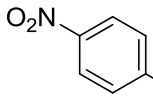
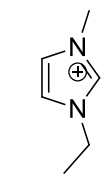
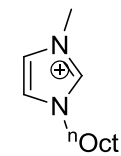
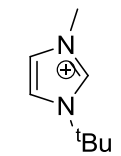
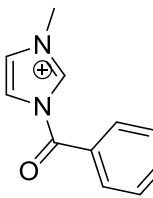
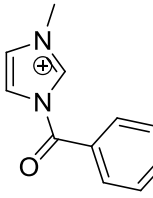
3.3.1 Calculation results: proton affinity

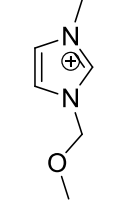
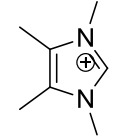
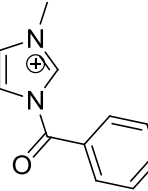
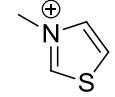
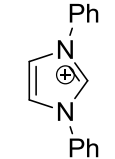
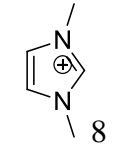


3.3.2 Calculation results: pK_a (Bartberger's method)

Table 3.1. Calculated gas-phase deprotonation energies (PA), solvation energies, and experimental and calculated pK_a values for imidazolium-like compounds in DMSO

compound	PA (calc, gas) kcal/mol B3LYP/6- 31+G*	pK _a (exp) in DMSO	$\Delta\Delta G_{\text{solvation}}^{\neq}$ Kcal/mol	PA (calc, PCM) (PA _{calc, gas} - $\Delta\Delta G_{\text{solvation}}$)	pK _a (calc)
	268.9	22.7 (23.2)	53.5	215.4	28.4
	265.6	24	50.8	214.8	26.5
	247.8	16.9	37.2	210.6	13.1
	242	16.9	36.1	205.9	-1.9

	246.9	17.8	35.0	211.9	17.2
	261.4	22.1	49.8	211.6	16.3
	263.1	22.1	49.9	213.2	21.4
	265.0	22.6	51.3	213.7	23.0
	256.3	21.6	41.3	215.0	27.1
	252.3	21.2	40.6	211.7	16.6

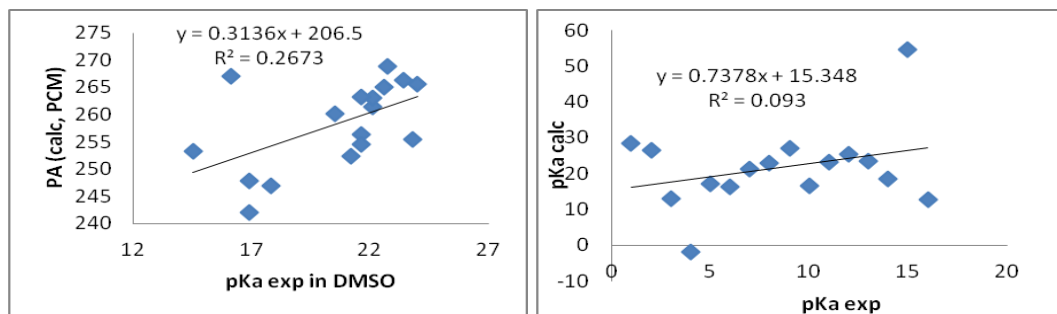
	260.2	20.5	46.4	213.8	23.3
	266.4	23.4	51.9	214.5	25.5
	254.5	21.6	40.6	213.9	23.6
	253.3	14.5	41.0	212.3	18.5
	267	16.1	43.4	223.6	54.5
	259.9	22.0 (21.1)	49.4	210.5	12.8

$\text{pK}_a(\text{exp})^{33, 34, 35, 36, 37, 38, 39, 40, 41}$

PA (calc, gas) B3LYP/6-31+G*

$\Delta\Delta G_{\text{solvation}}$ CPCM-B3LYP/6-31+G*// B3LYP/6-31+G*

The pK_a (calc) obtained from the linear regression plot $PA_{(calc, PCM)} = 0.3136 pK_a (calc) + 206$.

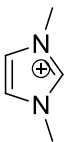
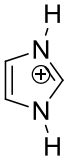
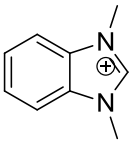


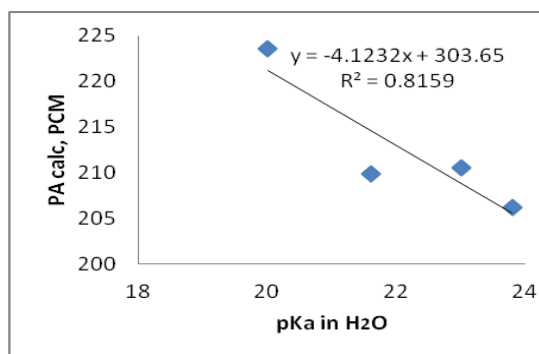
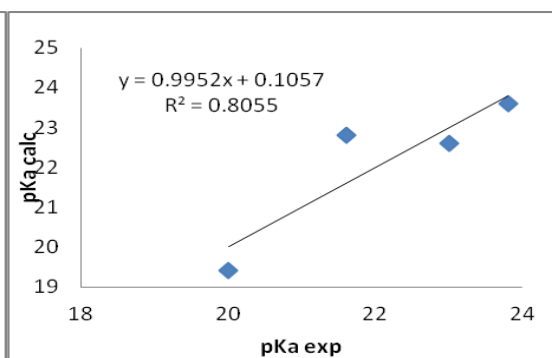
Plot1. $PA_{calc, PCM}$ vs pK_a (exp) in DMSO
(calc)

Plot2. pK_a (exp) in DMSO vs pK_a

Table 3.2. Calculated gas-phase deprotonation energies (PA), solvation energies, and experimental and calculated pK_a values for imidazolium-like compounds in H_2O

compound	PA (calc, gas) Kcal/mol B3LYP/6-31+G*	pK_a (exp) in H_2O	$\Delta\Delta G_{solvation}^\ddagger$ Kcal/mol	PA (calc, PCM) ($PA_{calc, gas} - \Delta\Delta G_{solvation}$)	pK_a (calc)
	267	20	43.4	223.6	19.4

	259.9	23	49.4	210.5	22.6
	255.5	23.8	49.3	206.2	23.6
	263.3	21.6	53.5	209.8	22.8

Plot3. $PA_{\text{calc, PCM}}$ vs pK_a in H_2O Plot4. pK_a (exp) in H_2O vs pK_a (calc)

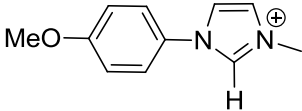
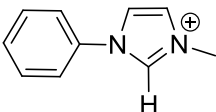
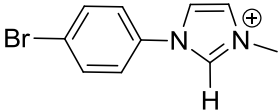
pK_a (exp) ^{42, 43,44,45,46,47,48,49,50}

PA (calc, gas) B3LYP/6-31+G*

$\Delta\Delta G_{\text{solvation}}$ CPCM-B3LYP/6-31+G*// B3LYP/6-31+G*

$PA_{\text{(calc, PCM)}} = -4.1232 pK_a(\text{calc}) + 303.65$

Table 3.3 Calculated pK_a of Strassner's carbenes by applying Bartberger's method

Strassner's carbenes	$\Delta\Delta G_{\text{solvation}}^{\neq}$ Kcal/mol	PA (calc, PCM)	pK _a (calc) in DMSO	pK _a (calc) in H ₂ O
 264.2 kcal/mol	49.7	214.5	25.5	21.6
 261.4 kcal/mol	48.9	212.5	19.1	22.1
 258.4 kcal/mol	47.7	210.7	22.5	22.5

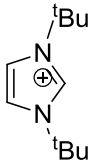
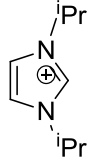
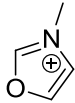
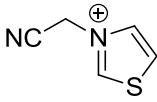
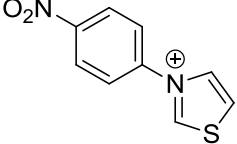
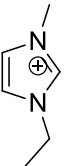
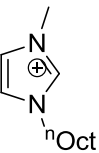
$$\text{pK}_a(\text{calc}) = (\text{PA}(\text{calc}, \text{PCM}) - 206.5) / 0.3136 \text{ in DMSO}$$

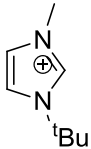
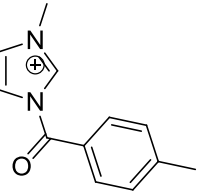
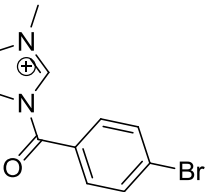
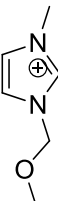
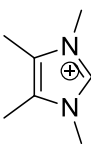
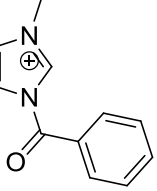
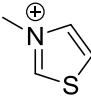
$$\text{pK}_a(\text{calc}) = (\text{PA}(\text{calc}, \text{PCM}) - 303.65) / (-4.1232) \text{ in H}_2\text{O}$$

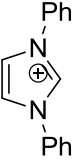
3.3.3 Calculation results: pK_a (Ogretir's method)

Table 3.4 Calculated gas phase proton affinity (PA), solvation free energies of ionization (ΔG_a), and experimental and calculated pK_a values in DMSO

compound	PA (calc, gas) kcal/mol	pK _a (exp) in DMSO	ΔG_a Kcal/mol	pK _a (calc) (ΔG_a)/1.36	pK _a (estd) in
----------	----------------------------	----------------------------------	--------------------------	---	------------------------------

	B3LYP/6-31+G*				DMSO
	268.9	22.7 (23.2)	50.0	36.8	23.4
	265.6	24	47.4	34.8	22.5
	247.8	16.9	33.7	24.8	17.7
	242	16.9	32.7	24.0	17.3
	246.9	17.8	31.6	23.2	17.0
	261.4	22.1	46.3	34.0	22.1
	263.1	22.1	46.4	34.1	22.1

	265.0	22.6	47.8	35.1	22.6
	256.3	21.6	37.8	27.8	19.1
	252.3	21.2	37.1	27.3	18.9
	260.2	20.5	42.9	31.5	20.9
	266.4	23.4	48.4	35.6	22.8
	254.5	21.6	37.1	27.3	18.9
	253.3	14.5	37.6	27.6	19.0

	267	16.1	40.4	29.3	19.8
---	-----	------	------	------	------

pK_a (exp) in DMSO^{51, 52,53,54,55,56,57,58,59}

PA (calc, gas) B3LYP/6-31+G*

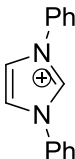
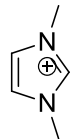
$\Delta\Delta G_{\text{solvation}}$ CPCM-B3LYP/6-31+G*// B3LYP/6-31+G*

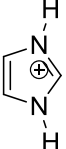
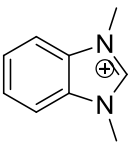
$\Delta G_a = \Delta G_g + \Delta G_s(B) - \Delta G_s(BH) + \Delta G_s(H^+) = \Delta G_g + \Delta G_s(B) - \Delta G_s(BH) - 259.5$

$pK_a(\text{calc}) = (\Delta G_a)/1.36$

$pK_a(\text{estd}) = 0.4763 * pK_a(\text{calc}) + 5.872$

Table 3.5 Calculated gas phase proton affinity (PA), solvation free energies of ionization (ΔG_a), and experimental and calculated pK_a values in H₂O

compound	PA (cal) Kcal/mol B3LYP/6-31+G*	pK_a (exp) in H ₂ O	ΔG_a Kcal/mol	pK_a (calc)	pK_a (estd) in H ₂ O
	267	20 ^f	40.4	29.3	16.8
	259.9	23 ^a	45.8	33.4	23.2

	255.5	23.8 ^a	46.0	33.8	23.8
	263.3	21.6 ^a	42.7	31.4	20.1

pK_a (exp) in DMSO ^{a-i}

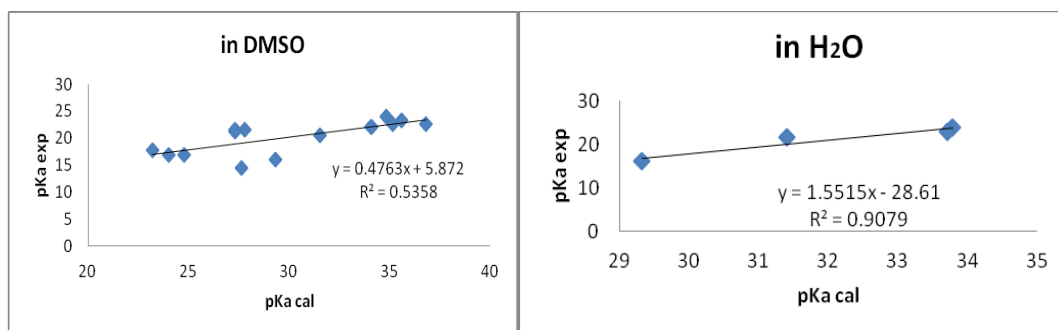
PA (calc, gas) B3LYP/6-31+G*

$\Delta\Delta G_{\text{solvation}}$ CPCM-B3LYP/6-31+G*// B3LYP/6-31+G*

$\Delta G_a = \Delta G_g + \Delta G_s(B) - \Delta G_s(BH) + \Delta G_s(H^+) = \Delta G_g + \Delta G_s(B) - \Delta G_s(BH) - 259.5$

$pK_a(\text{calc}) = (\Delta G_a)/1.36$

$pK_a(\text{estd}) = 1.5515 * pK_a(\text{calc}) - 28.61$

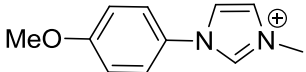
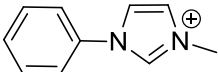
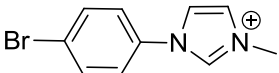


Plot 5 Relation between pK_a (exp) and pK_a (calc) Plot 6 Relation between pK_a (exp) and pK_a (calc)

in DMSO

in H₂O

Table 3.6 Calculated pK_a of Stassner's carbenes by applying Ogretir's method

Strassner's carbene	ΔG_a Kcal/mol	PA (calc, gas)	pK _a (calc)	pK _a (estd) in DMSO	pK _a (estd) in H ₂ O
 264.2 kcal/mol B3LYP/6-31+G* 300.9 kcal/mol bp86/6-311+G(d,p)	43.5	214.5	32.0	21.1	21.0
 261.4 kcal/mol B3LYP/6-31+G* 302.1 kcal/mol bp86/6-311+G(d,p)	42.7	212.5	31.5	20.8	20.3
 258.4 kcal/mol B3LYP/6-31+G* 300.9 kcal/mol bp86/6-311+G(d,p)	41.5	210.7	30.5	20.4	18.7

$$pK_a \text{ (estd) in DMSO} = 0.4763 * pK_a \text{ (calc)} + 5.872$$

$$pK_a \text{ (estd) in H}_2\text{O} = 1.5515 * pK_a \text{ (calc)} - 28.61$$

3.3.4 Experimental results: proton affinity

Table 3.7 Summary of proton affinity of 1-(4-methoxyphenyl)-3-methyl-1H-imidazol-3-ium

		Proton Transfer	PA (exp)
--	--	-----------------	----------

Ref. Compound	Proton Affinity (kcal/mol)	Ref. base	Conjugate acid	
tBuP ₁ (dma)	260.6	-	NA	PA>263.8 kcal/mol
tOctP ₁ (dma)	262.0	-	NA	
BEMP	263.8	-	NA	

Table 3.8 Summary of proton affinity of 3-methyl-1-phenyl-1H-imidazol-3-ium

Ref. Compound	Proton Affinity (kcal/mol)	Proton Transfer		PA (exp)
		Ref. base	Conjugate acid	
DBU	250.5	-	NA	PA=261.3±3 kcal/mol
MTBD	254.0	-	NA	
HP ₁ (dma)	257.0	-	NA	
tBuP ₁ (dma)	260.6	-	NA	
tOctP ₁ (dma)	262.0	+	NA	
BEMP	263.8	+	NA	

Table 3.9 Summary of proton affinity of 1-(4-bromophenyl)-3-methyl-1H-imidazol-3-ium

Ref. Compound	Proton Affinity (kcal/mol)	Proton Transfer		PA (exp)
		Ref. base	Conjugate acid	

DBU	250.5	-	NA	PA=258.8±3 kcal/mol
MTBD	254.0	-	NA	
HP ₁ (dma)	257.0	-	NA	
tBuP ₁ (dma)	260.6	+	NA	
tOctP ₁ (dma)	262.0	+	NA	
BEMP	263.8	+	NA	

3.4 Discussion & Conclusion

We used three methods to predict the pK_a of Strassner's carbenes.

Method 1: Relation between PA (calc, gas) and pK_a (exp)

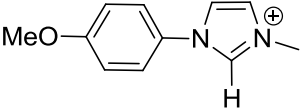
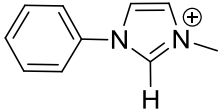
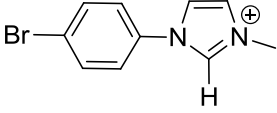
Method 2: Relation between PA (calc, PCM) and pK_a (exp) -- Bartberger method

Method 3: Relation between pK_a (calc) and pK_a (exp) – We followed Ogretir's method

For predicting pK_a of imidazolium compound in H₂O, all three methods produce plots with good R² values, implying the pK_a prediction is good.

Method 1 is relatively reliable for predicting the pK_a of imidazolium compound in DMSO, based on the linearity of the plot. Although R² value is 0.35, there are two outliers. However, this method does not take any solvation energy into consideration. Method 2 is very unreliable for predicting the pK_a of imidazolium compound in DMSO, in the sense that the plot has a very low R² value and all the points are scattered. Method 3 is the most reliable method so far, with a plot that has an R² value 0.54. It also takes the solvation energy into consideration.

Table 3.10 Calculated pKa of Stassner's carbenes by applying Method 1-3

Strassner's carbenes	Method 1	Method 2	Method 3
 264.2 kcal/mol	21.7 in DMSO 21.2 in H ₂ O	25.5 in DMSO 21.6 in H ₂ O	21.1 in DMSO 21.1 in H ₂ O
 261.4 kcal/mol	21.1 in DMSO 22.1 in H ₂ O	19.1 in DMSO 22.1 in H ₂ O	20.8 in DMSO 20.3 in H ₂ O
 258.4 kcal/mol	20.4 in DMSO 23.1 in H ₂ O	22.5 in DMSO 22.5 in H ₂ O	20.4 in DMSO 18.7 in H ₂ O

Chapter 4 Stabilized carbene project

4.1 Introduction

NHCs are effective ligands of 2nd generation catalyst for Grubbs ruthenium olefin metathesis⁶⁰, which is more active than the 1st generation of catalyst (Figure 4.1)^{61,62}.

Presumably the ligands are more effective if they are more basic. In addition, the only differences between the 2nd and 1st generation Grubbs catalyst is that the Ru is replaced with N-heterocyclic singlet carbene instead of PCy₃. Therefore, it would be interesting to compare the proton affinity of NHCs and PCy₃.

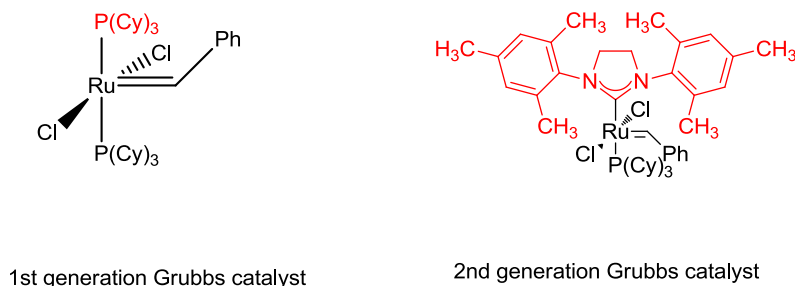


Figure 4.1 Structures of Grubbs catalysts

We compare the proton affinity (PA) of imidazole-2-ylidenes and tricyclohexylphosphine (PCy₃) with Cooks Kinetic Method on a linear trap quadrupole mass spectrometer (LTQ). However, an ion with $m/z=295$ was also observed in addition to the protonated carbene and protonated phosphine. There are two pathways to generate the ion with $m/z=295$, one is by elimination (Figure 4.2, pathway A) and the other is by substitution (Figure 4.2, pathway B).

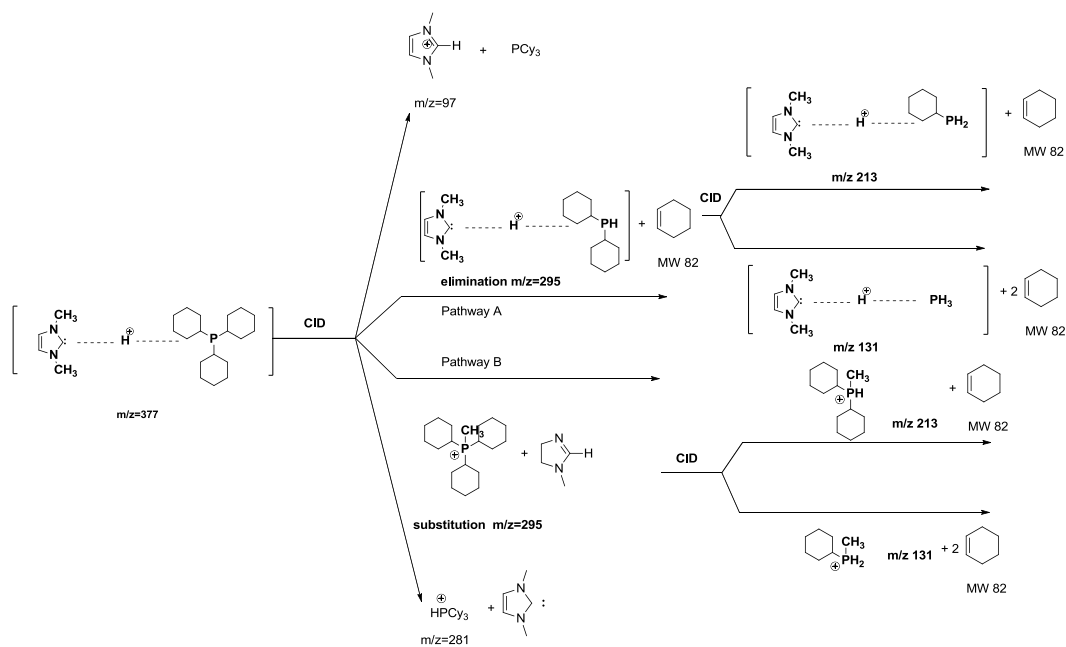


Figure 4.2 Elimination and substitution pathway for di-methylimidazolium*phosphine dimer

To find out exactly which pathway the dimer will go with, we designed and synthesized the di- CD_3 carbene derivative, from which we could differentiate the elimination and substitution pathways (Figure 4.3).

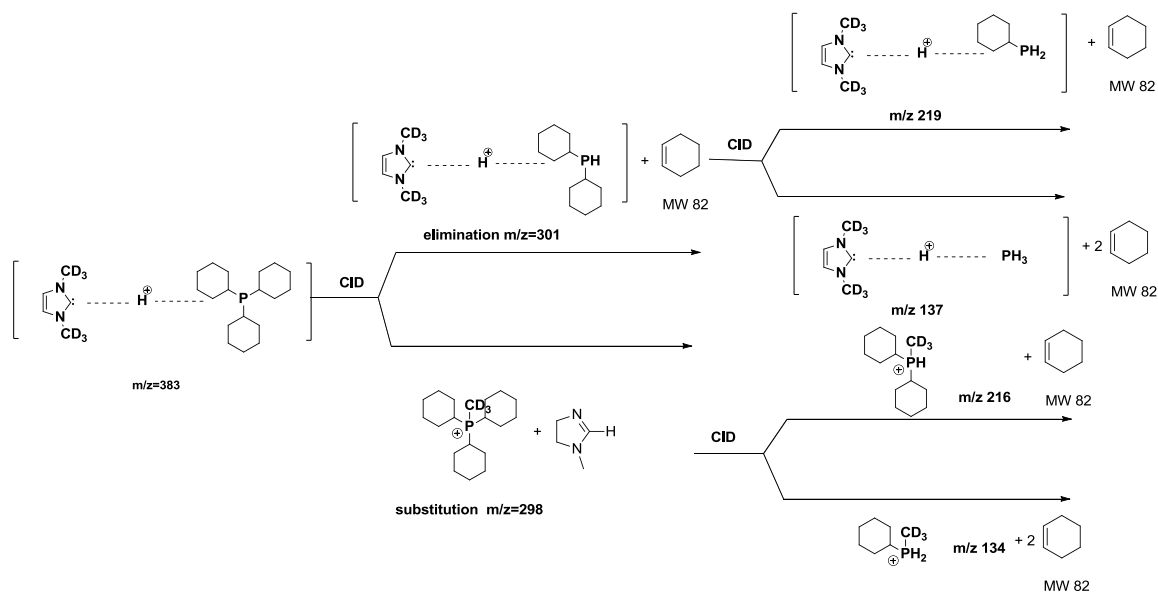
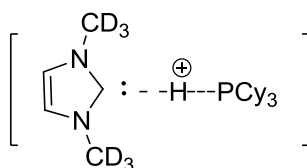


Figure 4.3 Elimination and substitution pathway for di- CD_3 -imidazolium*phosphine dimer

4.2 Experimental

All chemicals are commercially available except for di- CD_3 -imidazolium salt, which was synthesized following literature procedure⁶³. Methanol was degassed by nitrogen for 30 min before use. All the solutions are prepared in the glove box, and then protected by N_2 .

To investigate the oxidation of tricyclohexylphosphine (PCy_3) and protonated dimethylimidazolium •phosphine dimer, 0.5mM solution in methanol was electrosprayed in the quadrupole ion trap mass spectrometer (Thermo Finnigan LCQ) with a needle voltage of 5 kV, capillary temperature of 100°C and a flow rate of $25\mu\text{L}/\text{min}$. The fullscan at 0, 10, 15, 20, 30, 45, 60 min were taken to study the oxidation of PCy_3 with time.



4.3 Results

The oxidation of phosphine was well controlled after all the solutions were prepared in the glove box and protected by N₂. About 20% intensity of protonated oxidized phosphine (m/z=297) was observed after the experiment was performed for 20 min (Figure 4.5).

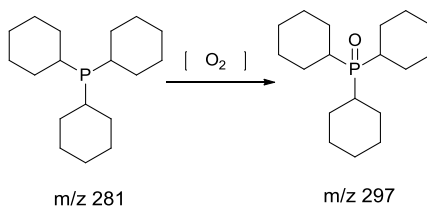


Figure 4.5 Oxidation of phosphine

The studies on the protonated di-CD₃-imidazolium •phosphine dimer yielded an ion at m/z 298, which corresponds to the CD₃PCy₃ upon CID. The results showed that the dimer reacted via the substitution pathway instead of cyclohexene elimination (no m/z 301 ion). Subsequent CID on the m/z 298 ion produced ions with m/z 216 and m/z 134, which correspond to the loss of one and two cyclohexene. (Figure 4.6)

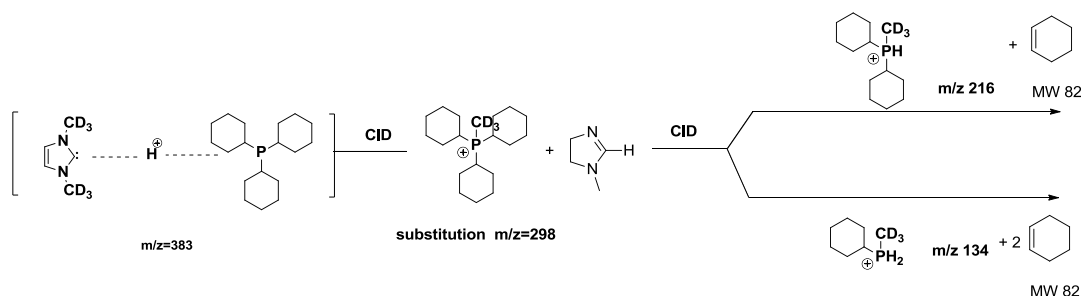


Figure 4.6 Substitution pathway for di-CD₃-imidazolium*phosphine dimer

4.4 Conclusion

We have probed interesting reactivity that the proton bound dimers of di-methyl-imidazolium salt and di-CD₃-imidazolium salt with PCy₃ display upon CID. The dimethyl system undergoes phosphine methylation.

Reference:

- ¹ De Hoffmann, E.; Charrette, J.; Stroobant, V. *Mass Spectrometry Principles and Applications*; John Wiley&Sons: Chichester, 1999.
- ² *NIST Chemistry WebBook, Nist Standard Reference Database Number 69*, June 2005; Linstrom, P. J.; Mallard, W. G., Eds.; National Institutent of Atandards and Technology: Gaithersburg, MD 20899, 2005; <http://webbook.nist.gov>.
- ³ Sharma, S.; Lee, J. K. *J. Org. Chem.* 2002, 67, 8360-8365
- ⁴ Sharma, S.; Lee, J. K. *J. Org. Chem.* 2004, 69, 7018-7025.
- ⁵ Zhachkina, A.; lee, J. K. *J. Am. Chem. Soc.* 2009, 131, 18376–18385.
- ⁶ Oldamur H.; Terleczyk, P.; Szieberth, D.; Mourgas, G.; Gudat, D. *J. Am. Chem. Soc.* 2011, 133, 780–789.
- ⁷ Enders, D.; Niemeier, O.; Henseler, A. *Chem. Rev.* 2007, 107, 5606-5655.
- ⁸ Struble, J. R.; Kaeobamrung, J.; Bode, J. W. *Org. Lett.* 2008, 10, 957-960.
- ⁹ Trnka, T. M.; Grubbs, R. H. *Acc. Chem. Res.* 2001, 34, 18-29.
- ¹⁰ Ahrens, S.; Peritz, A.; Strassner, T. *Angew. Chem. Int. Ed.* 2009, 48, 7908-2910.
- ¹¹ Amster, I. J. *J. Mass Spectrom.* 1996, 31, 1325-1337.
- ¹² Marshall, A. G.; Grosshans, P. B. *Anal. Chem.* 1991, 63A, 215-229.
- ¹³ Comisarow, M. B.; Marshall, A. G. *Chemical Physics Letters* 1974, 25, 282-283.
- ¹⁴ Sanz-Medel, A. *Analyst* 2000, 125, 35-43.
- ¹⁵ March, R. E. *Quadrupole Ion Trap Mass Spectrometer*; John Wiley & Sons Ltd: Chichester, 2000.
- ¹⁶ Douglas, D. J.; Frank, A. J.; Mao, D. *Mass Spectrometry Reviews* 2005, 24, 1-29.
- ¹⁷ Cooks, R. G.; Kruger, T. L. *J. Am. Chem. Soc.* 1977, 99.
- ¹⁸ MuLucky, S. A.; Cameron, D.; Cooks, R. G. *J. Am. Chem. Soc.* 1981, 103, 1313-1317.
- ¹⁹ Brodbelt-Lustig, J. S.; Cooks, R. G. *Talanta* 1989, 36, 255-260.
- ²⁰ Green-Church, K. B.; Limbach, P. A. *J. Am. Chem. Soc. Mass Spectrom.* 2000, 11, 24-32.
- ²¹ Frisch, R. C.; al., e. *Gaussian03, Rev. C.*; Gaussian Inc: Wallingford, CT, 2004.

-
- ²² Barone, V.; Cossi, M. *J. Phys. Chem. A* **1998**, *102*, 1995-2001.
- ²³ Cossi, M.; Rega, N.; Scalmani, G.; Barone, V. *J. Comput. Chem.* **2003**, *24*, 669-681.
- ²⁴ Kavli, B.; Otterlei, M.; Slupphaug, G.; Krokan, H. E. *DNA Repair* **2007**, *6*, 505-516.
- ²⁵ Connolly, B. A.; Fogg, M. J.; Shuttleworth, G.; Wilson, B. T. *Biochem. Soc. Trans.* **2003**, *31*, 699-702.
- ²⁶ Parker, J. B.; Bianchet, M. A.; Krosky, D. J.; Friedman, J. I.; Amzel, L. M.; Stivers, J. T. *Nature* **2007**, *449*, 433-438.
- ²⁷ Bellamy, S. R. W.; Krusong, K.; Baldwin, G. S. *Nucleic Acids Res.* **2007**, *35*, 1478-1487.
- ²⁸ Savva, R.; McAuley-Hecht, K.; Brown, T.; Pearl, L. *Nature* **1995**, *373*, 487-493.
- ²⁹ Chankeshwara, S.; Chakraborti, A. *Org. Lett.* **2006**, *8*, 3259-3262.
- ³⁰ Arduengo, A. J. I.; Goerlich, J. R.; Marshall, W. J. *J. Am. Chem. Soc.* **1991**, *113*, 361-363.
- ³¹ Igau, A.; Baceiredo, A.; Trinquier, G.; Bertrand, G. *Angew. Chem. Int. Ed. Engl.* **1989**, *101*, 617-618.
- ³² Oldamur H.; Terleczyk, P.; Szieberth, D.; Mourgas, G.; Gudat, D. *J. Am. Chem. Soc.* **2011**, *133*, 780-789.
- ³³ Amyes, T.; Diver, S.; Richard, J.; Rivas, F.; Toth, K. *J. Am. Chem. Soc.* **2004**, *126*, 4366.
- ³⁴ Washabaugh, M.; Jencks, W. *Biochemistry* **1988**, *27*, 5044-5053.
- ³⁵ Robinson, D. *J. Am. Chem. Soc.* **1970**, *92*, 3138-3146.
- ³⁶ Haake, P.; Bausher, L. *J. Phys. Chem.*, **1968**, *72*, 2213.
- ³⁷ Droge, T.; Glorius, F. *Angew. Chem. Int. Ed.* **2010**, *49*, 6940 - 6952.
- ³⁸ Magill, A.; Cavell, K.; Yates, B. *J. Am. Chem. Soc.* **2004**, *126*, 8717.
- ³⁹ Chu, Y.; Deng, H.; Cheng, J. *J. Org. Chem.* **2007**, *72*, 7790.
- ⁴⁰ Haake, P.; Bausher, L.; Miller, W. *J. Am. Chem. Soc.* **1969**, *91*, 1112-1119.
- ⁴¹ Chu, Y.; Deng, H.; Cheng, J. *J. Org. Chem.* **2007**, *72*, 7790-7793.
- ⁴² Amyes, T.; Diver, S.; Richard, J.; Rivas, F.; Toth, K. *J. Am. Chem. Soc.* **2004**, *126*, 4366.
- ⁴³ Washabaugh, M.; Jencks, W. *Biochemistry* **1988**, *27*, 5044-5053.

-
- ⁴⁴ Robinson, D. *J. Am. Chem. Soc.* **1970**, 92, 3138-3146.
- ⁴⁵ Haake, P.; Bausher, L. *J. Phys. Chem.*, **1968**, 72, 2213.
- ⁴⁶ Droge, T.; Glorius, F. *Angew. Chem. Int. Ed.* **2010**, 49, 6940 – 6952.
- ⁴⁷ Magill, A.; Cavell, K.; Yates, B. *J. Am. Chem. Soc.* **2004**, 126, 8717.
- ⁴⁸ Chu, Y.; Deng, H.; Cheng, J. *J. Org. Chem.* **2007**, 72, 7790.
- ⁴⁹ Haake, P.; Bausher, L.; Miller, W. *J. Am. Chem. Soc.* **1969**, 91, 1112-1119.
- ⁵⁰ Chu, Y.; Deng, H.; Cheng, J. *J. Org. Chem.* **2007**, 72, 7790-7793.
- ⁵¹ Amyes, T.; Diver, S.; Richard, J.; Rivas, F.; Toth, K. *J. Am. Chem. Soc.* **2004**, 126, 4366.
- ⁵² Washabaugh, M.; Jencks, W. *Biochemistry* **1988**, 27, 5044-5053.
- ⁵³ Robinson, D. *J. Am. Chem. Soc.* **1970**, 92, 3138-3146.
- ⁵⁴ Haake, P.; Bausher, L. *J. Phys. Chem.*, **1968**, 72, 2213.
- ⁵⁵ Droge, T.; Glorius, F. *Angew. Chem. Int. Ed.* **2010**, 49, 6940 – 6952.
- ⁵⁶ Magill, A.; Cavell, K.; Yates, B. *J. Am. Chem. Soc.* **2004**, 126, 8717.
- ⁵⁷ Chu, Y.; Deng, H.; Cheng, J. *J. Org. Chem.* **2007**, 72, 7790.
- ⁵⁸ Haake, P.; Bausher, L.; Miller, W. *J. Am. Chem. Soc.* **1969**, 91, 1112-1119.
- ⁵⁹ Chu, Y.; Deng, H.; Cheng, J. *J. Org. Chem.* **2007**, 72, 7790-7793.
- ⁶⁰ Taige, M.; Zeller, A.; Ahrens, S.; Goutal, S.; Herdtweck, E.; Strassner, T. *J. Organometallic. Chem.* **2007**, 692, 1519-1529.
- ⁶¹ Enders, D.; Niemeier, O.; Henseler, A. *Chem. Rev.* **2007**, 107, 5606-5655.
- ⁶² Struble, J. R.; Kaeobamrung, J.; Bode, J. W. *Org. Lett.* **2008**, 10, 957-960.
- ⁶³ Zhao, H.; Foss, F. W.; Breslow, R. *J. Am. Chem. Soc.* **2008**, 130, 12590-12591.

CURRICULUM VITAE

Sisi Zhang

Education:

2005-2009 B.S., Pharmaceutical Sciences

Peking University, P. R. China

2009 - 2012 M.S., Chemistry and Chemical Biology

Rutgers, The State University of New Jersey

Publications:

Liu, M.; Chen, M.; **Zhang, S.** Yang, I.; Buckley, B.; Lee, J. K. "Reactivity of Carbene•Phosphine Dimers: Proton Affinity Revisited," *J. Phys. Org. Chem.* ASAP